Geological Magazine

www.cambridge.org/geo

Original Article

Cite this article: Saraswat R, Rajput KR, Bandodkar SR, Bhadra SR, Kurtarkar SR, Maria Joäo H, Suokhrie T, and Kumar P (2023) Persistent increase in carbon burial in the Gulf of Mannar, during the Meghalayan Age: Influence of primary productivity and better preservation. *Geological Magazine* **160**: 561–578. https://doi.org/10.1017/S001675682200111X

Received: 3 January 2022
Revised: 2 October 2022
Accepted: 4 October 2022
First published online: 9 January 2023

Keywords:
carbon; calcium carbonate; organic matter; Gulf of Mannar; Meghalayan Age

Author for correspondence:
Rajeev Saraswat, Email: rsaraswat@nio.org

Persistent increase in carbon burial in the Gulf of Mannar, during the Meghalayan Age: Influence of primary productivity and better preservation

Rajeev Saraswat[1], Karan Rampal Rajput[1,2], Sripad Rohidas Bandodkar[1], Sudhir Ranjan Bhadra[1], Sujata Raikar Kurtarkar[1], Hilda Maria Joäo[1], Thejasino Suokhrie[1] and Pankaj Kumar[3]

[1]Micropaleontology Laboratory, Geological Oceanography Division, CSIR–National Institute of Oceanography, Goa, India; [2]Karamshibhai Jethabhai Somaiya College, Mumbai University, Mumbai, India and [3]Inter University Accelerator Center, Delhi, India

Abstract

The oceans store a substantial fraction of carbon as calcium carbonate ($CaCO_3$) and organic carbon (C_{org}) and constitute a significant component of the global carbon cycle. The C_{org} and $CaCO_3$ flux depends on productivity and is strongly modulated by the Asian monsoon in the tropics. Anthropogenic activities are likely to influence the monsoon and thus it is imperative to understand its implications on carbon burial in the oceans. We have reconstructed multi-decadal $CaCO_3$ and C_{org} burial changes and associated processes during the last 4.9 ky, including the Meghalayan Age, from the Gulf of Mannar. The influence of monsoon on carbon burial is reconstructed from the absolute abundance of planktic foraminifera and relative abundance of *Globigerina bulloides*. Both C_{org} and $CaCO_3$ increased throughout the Meghalayan Age, except between 3.0–3.5 ka and the last millennium. The increase in C_{org} burial during the Meghalayan Age was observed throughout the eastern Arabian Sea. The concomitant decrease in the C_{org} to nitrogen ratio suggests increased contribution of marine organic matter. Although the upwelling was intense until 1.5 ka, the lack of a definite increasing trend suggests that the persistent increase in C_{org} and $CaCO_3$ during the early Meghalayan Age was mainly driven by higher productivity during the winter season coupled with better preservation in the sediments. Both the intervals (3.0–3.5 ka and the last millennium) of nearly constant carbon burial coincide with a steady sea-level. The low carbon burial during the last millennium is attributed to the weaker-upwelling-induced lower productivity.

1. Introduction

Carbon dioxide (CO_2) and methane (CH_4) are the two dominant gaseous forms of carbon in the atmosphere. The atmospheric CO_2 concentration depends on a multitude of processes involving the exchange of carbon between atmosphere, lithosphere, oceans and biosphere, collectively defined as the global carbon cycle (Carlson *et al.* 2001). The excessive use of fossil fuels (coal, petroleum) since industrialization has increased the atmospheric CO_2 concentration to levels unprecedented in the last ~800 000 years (Lüthi *et al.* 2008). The atmospheric CO_2 combines with rainwater to form weak carbonic acid that dissolves rocks on the earth's surface. The dissolution of rocks, termed as silicate weathering, releases calcium and bicarbonate ions from the rocks into the rivers and subsequently into the oceans (Misra & Froelich, 2012). The silicate weathering is one of the significant components of the global carbon cycle, on longer timescales (Brady, 1991; Raymo & Ruddiman, 1992; Wan *et al.* 2012).

In the oceans, calcareous organisms combine calcium ions with bicarbonate ions to form calcium carbonate ($CaCO_3$) (Zeebe & Wolf-Gladrow, 2001). In modern oceans, most of the $CaCO_3$ is precipitated as the shells of microorganism, like foraminifera, coccolithophores and corals (Ramaswamy & Nair, 1994; Schiebel, 2002). Foraminifera, single-celled organisms with hard outer shells called test, contribute a significant fraction of the marine carbonate flux (Langer, 2008). After the death of the organisms, the shells sink to the ocean floor. Foraminiferal tests are usually constructed either by secreting $CaCO_3$ or by cementing sand, silt and other particles, known as agglutinated tests (Kaminski & Kuhnt, 1995; Saraswat, 2015; Saalim *et al.* 2019). Foraminiferal shells are one of the most abundant and significant fossil remains in marine sediments. In addition to the biogenic carbonate, organic matter also removes a substantial fraction of carbon from the ocean water and buries it in the sediments, as carbon is the main component of all life forms (Ciais *et al.* 2013). The photosynthesizing plants, collectively termed as marine productivity or marine primary productivity, constitute a substantial part of the oceanic organic matter (Field *et al.* 1998). Thus, the long-term carbon burial in the oceans includes both the organic carbon (C_{org}) and $CaCO_3$ in the sediments. Therefore, oceans are vital in modulating the global carbon cycle by regulating the amount of carbon buried in the sediments (Falkowski *et al.* 2000).

The anthropogenic greenhouse-gas-emission-induced warming is likely to affect the marine organisms and thus their contribution to carbon cycling. However, the likely response of the marine carbon cycling to the anthropogenic greenhouse-gas-emission-induced warming is not clear. Because of the unprecedented increase in atmospheric CO_2 concentration during the last ~150 years, it is crucial to understand its effect on marine carbon cycling. The carbon burial records from the oceans, covering the times of different atmospheric CO_2 concentrations in the past, can help understand the effects of anthropogenic contribution in global carbon cycling (Falkowski *et al.* 2000). The large influence of anthropogenic activities on global CO_2 supposedly began after the industrial revolution (IPCC, 2021). Therefore, long-term multi-decadal records of carbon burial, spanning the interval before significant anthropogenic activities, are required to understand the effect of human-induced perturbations on the carbon cycle.

The tropical Indian Ocean has a considerable carbon burial potential as its several regions have high primary productivity during the summer and winter monsoon (Prell & Curry, 1981; Prasanna Kumar *et al.* 2001; Sreeush *et al.* 2018). The northern Indian Ocean has the highest flux of inorganic ($CaCO_3$) and particulate organic carbon (Sarma *et al.* 2007). Many workers have documented the temporal changes in both the organic matter and $CaCO_3$ burial in the northern Indian Ocean and the processes affecting these changes (von Rad *et al.* 1999; Staubwasser & Sirocko, 2001; Reichart *et al.* 2002; Agnihotri *et al.* 2003*a*, *b*; Naik *et al.* 2014; Azharuddin *et al.* 2017; Naik *et al.* 2017). The monsoon-induced productivity, terrigenous influx by the rivers, grain size and bottom water conditions strongly influence the C_{org} and $CaCO_3$ content in the modern surface sediments of the Arabian Sea (Kolla *et al.* 1981; Galy *et al.* 2007). The large spatial heterogeneity observed in the distribution of C_{org} and $CaCO_3$ in the surface sediments of the Arabian Sea (Kolla *et al.* 1981; Paropkari *et al.* 1992) is also prevalent during the geologic past. The continuous increase in $CaCO_3$, biogenic opal, biogenic Ba and their mass accumulation rates throughout the Holocene in the SE Arabian Sea were attributed to higher productivity due to increased upwelling during the summer monsoon (Naidu, 1991; Thamban *et al.* 1997; Naidu & Shankar, 1999; Bhushan *et al.* 2001; Pattan *et al.* 2003). However, the decrease in $CaCO_3$ abundance in the NE Arabian Sea during the Holocene was attributed to terrigenous dilution (Naidu, 1991; Azharuddin *et al.* 2017). Interestingly, the relatively high C_{org} but low $CaCO_3$ in the SW margin of India during the late Holocene was attributed to increased productivity and diagenesis (Kessarkar & Rao, 2007). Although, the $CaCO_3$ content in the NE and mid-eastern Arabian Sea was more during the interglacial period, no specific variation was observed in the organic matter content during glacial and interglacial times (Guptha *et al.* 2005). A rapid decrease in productivity coeval with very low dissolved oxygen in the bottom waters during the Last Glacial Maximum was reported from the SE Arabian Sea (Naik *et al.* 2017). A strengthened winter monsoon during the Little Ice Age was inferred from the NE Arabian Sea (Böll *et al.* 2014). A consistent increase in C_{org} throughout the Meghalayan Age was attributed to increased sedimentation and better preservation under a more reducing environment (Nagoji & Tiwari, 2017). Interestingly, an altogether different pattern with higher C_{org} accumulation during the cold glacials and stadials as compared to low accumulation during the warmer interglacials and interstadials in the neighbouring Bay of Bengal was attributed to intense winter-monsoon-induced increased marine primary production during the colder intervals (Weber *et al.* 2018; Xu *et al.* 2021).

Therefore, a vast spatial variation is observed in both the organic matter and $CaCO_3$ burial in the Arabian Sea during the past, necessitating more regional records. The majority of previous studies focused on carbon burial changes during the glacial–interglacial interval. High-resolution carbon burial studies focused on the Holocene are limited. Additionally, the sample resolution in the majority of previous studies was too coarse to understand short-term carbon burial changes in the northern Indian Ocean. Therefore, the objective of this work was to reconstruct the multi-decadal carbon burial changes from the Gulf of Mannar during the last ~5000 years covering the Meghalayan Age (4.2 ka to recent), and to understand the factors affecting carbon burial in this region.

2. Study area

The gravity core (SSD004 GC02) collected from the upper slope of the Gulf of Mannar, off the southern tip of India (8° 37.9443′ N, 78° 44.1874′ E), during the fourth cruise of RV *Sindhu Sadhana* (October 2014) was used (Fig. 1). The core was retrieved from a depth of 1002 m. The study area is between the west coast of Sri Lanka and the southeast coast of India. The oceanographic processes mainly control the salinity, as except for the only perennial river of Tamil Nadu, namely the Thamirabarani River, no significant rivers drain directly into the Gulf of Mannar. A sizable seasonal change is observed in both the seawater temperature (varying from a lowest of 26.6°C during the summer monsoon season to a highest of 28.5°C during the pre-summer-monsoon season, in the top 25 m of the water column) (Locarnini *et al.* 2018) and salinity (varying from a lowest of 33.8 psu during the post-summer-monsoon season to the highest of 35.0 psu during the summer season, in the top 25 m of the water column) (Zweng *et al.* 2018). The changes are, however, restricted to the top ~200 m of the water column, and the deeper waters are relatively stable (Locarnini *et al.* 2018; Zweng *et al.* 2018; Fig. 2). The hydrography of the area is controlled mainly by the monsoon system. The mean annual rainfall varies from 760 mm to 1270 mm (Sulochanan & Muniyandi, 2005). The study area receives copious rainfall during both the summer and winter monsoon. The summer monsoon occurs from June to September and the winter monsoon occurs from October to November. The summer monsoon brings more rainfall as compared to the winter monsoon (Gadgil & Kumar, 2006). The seasonal reversal of winds results in considerable variation in the intensity of upwelling as well as the primary productivity (Haake *et al.* 1993). The upwelling increases productivity in the area during May–June (Thomas *et al.* 2013). The Ekman Pumping induces large phytoplankton bloom increasing the chlorophyll-*a* content (up to 2 mg m^{-3}) in the SW Bay of Bengal during the winter monsoon season (Vinayachandran & Mathew, 2003). The high-productivity water advects into the Gulf of Mannar from the Palk Bay during the winter season, increasing the productivity

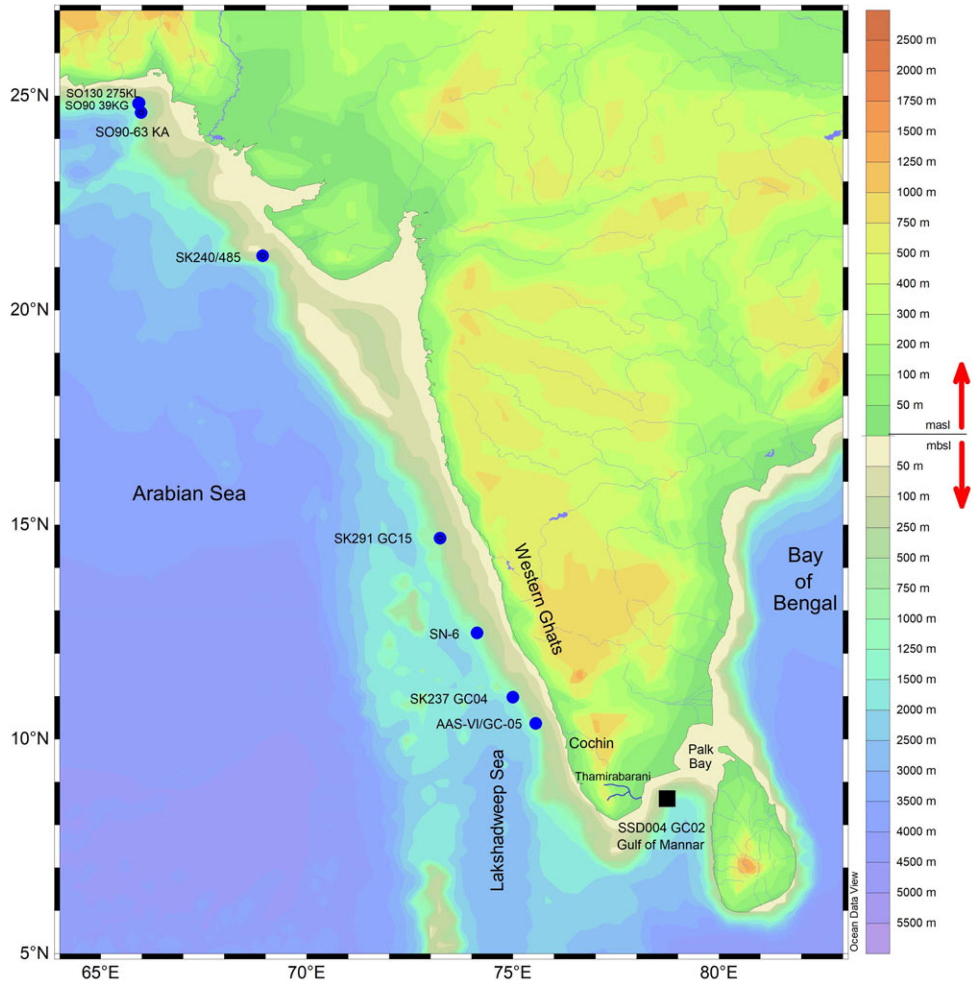

Fig. 1. (Colour online) The core location and other cores from the eastern Arabian Sea (SO90-39 KG/SO130-275 KL, Böll *et al.* 2014; SO90-63 KA, Burdanowitz *et al.* 2019; SK240/485, Azharuddin *et al.* 2017; SK291 GC15, Saravanan *et al.* 2019; SN-6, Nagoji & Tiwari, 2017; AAS-VI/GC-05, Pattan *et al.* 2019; SK237 GC04, Naik *et al.* 2017) discussed in the paper. The filled black square is the location of core SSD004 GC02 in the Gulf of Mannar. The coloured contours are bathymetry/topography and the scale is on the right. The major bathymetric and topographic features and Thamirabarani River are also marked. The faint blue lines mark the major rivers draining in the northern Indian Ocean.

(Jyothibabu *et al.* 2021). The large influx from the rivers draining into the Gulf of Mannar also increases the nutrient availability and, in turn, productivity during the winter season (Chandramohan *et al.* 2001). The zooplankton biomass and chlorophyll-*a* concentration during the winter season is comparable with that during the summer season in the Gulf of Mannar (Jagadeesan *et al.* 2013). The seasonally reversing winds generate coastal currents that transport warm saltier water from the Arabian Sea into the Bay of Bengal during the summer, and cold fresher water from the Bay of Bengal into the Arabian Sea during the winter (Schott & McCreary, 2001).

The region has an extensive relict carbonate platform, with the age of the overlying sediments varying from 7.3 to 8.4 ka (Rao *et al.* 2003). The sediments are sandy on the continental shelf, gradually dominated by the silt and clay on the slope and further deeper regions (Hashimi *et al.* 1981; 1982; Singh *et al.* 2018). The inner shelf sediments are dominated by $CaCO_3$ of biogenic origin (foraminifera, molluscs, pteropods) (Hashimi *et al.* 1982). The C_{org} in surface sediments varies from 1.5 % to 6.9 % (Singh *et al.* 2018). The dissolved oxygen varies from 0.48 mL L^{-1} to 3.84 mL L^{-1}, with the oxygen-deficient zone (<2 mL L^{-1}) between 152 and 1550 m (Singh *et al.* 2018). Based on the previous studies, sedimentation rate is comparatively high on the slope (Ray *et al.* 1990; Singh *et al.* 2017). Consequently, the core location was selected to ensure a high sedimentation rate record.

3. Materials and methodology

The core (SSD004 GC02) was 5.95 m long and the top 1.50 m section of the core was used for the study. The core was subsampled at 1 cm intervals and thus a total of 150 samples were used. The samples were processed in several stages.

3.1. Sample processing for foraminiferal studies

A small aliquot (5–10 g) of sediment was collected in a pre-weighed glass Petri dish and freeze-dried. The dried sediments were weighed and sieved using a 63 μm sieve. The material retained on the sieve (>63 μm, coarse fraction, CF) was dried, weighed and stored in clean plastic vials. For picking planktic foraminifera, one-quarter of the coarse fraction was weighed and dry-sieved using a 125 μm sieve. Both the >125 μm and <125 μm fractions were then weighed and stored in separate vials. A representative aliquot of >125 μm fraction was weighed and uniformly spread in a picking tray. A minimum of 300 completely intact planktic foraminifera tests were picked from this fraction using an

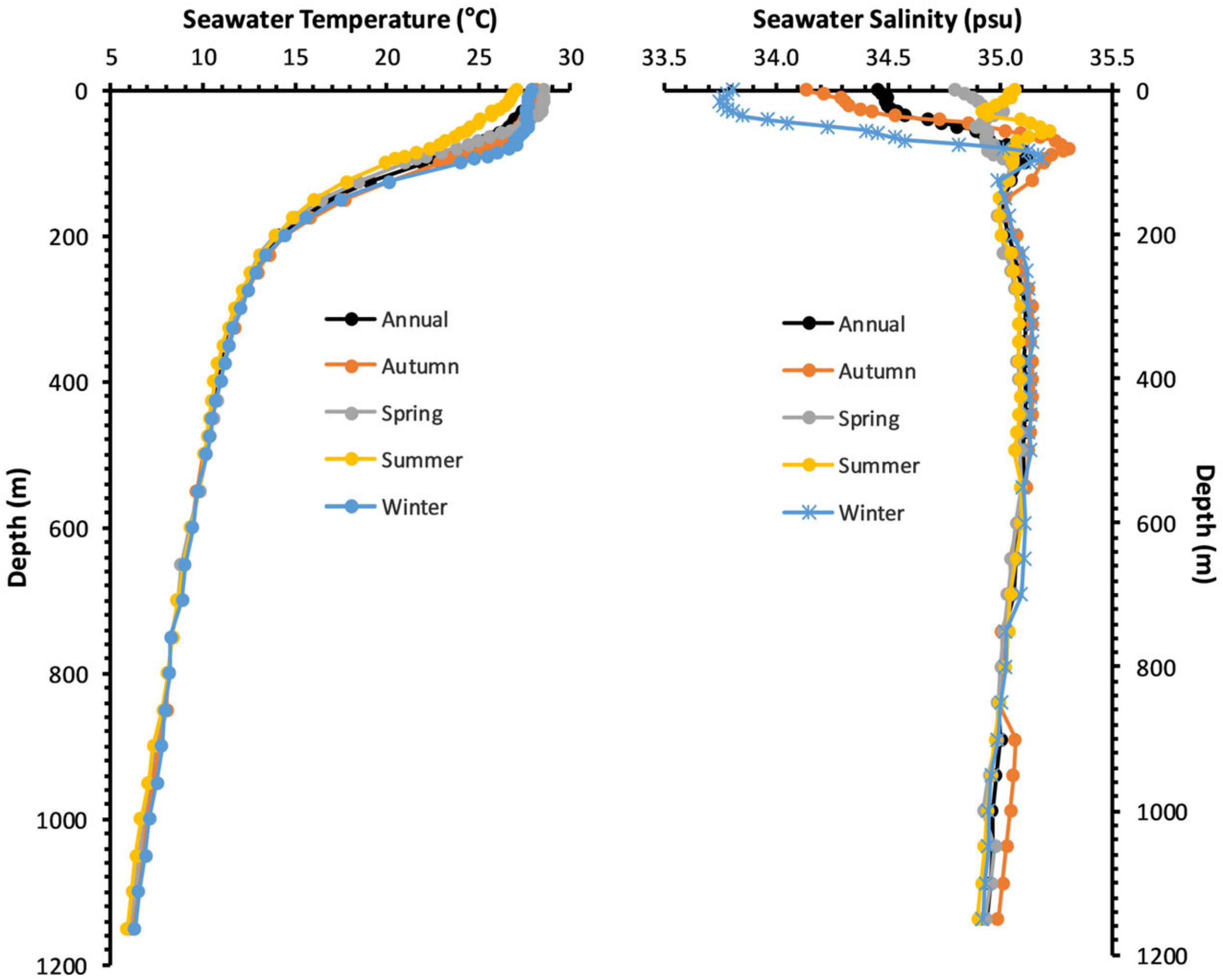

Fig. 2. (Colour online) Annual and seasonal water column temperature (Locarnini *et al.* 2018) and salinity (Zweng *et al.* 2018) at the core location.

Olympus SZX16 stereozoom microscope. Planktic foraminiferal abundance was normalized to 1 g dry sediment weight. The number of specimens of *Globigerina bulloides* was counted and its relative abundance was calculated.

3.2. Total carbon, nitrogen and inorganic carbon analysis

About 1–2 g of the freeze-dried sediment was finely powdered for the total and inorganic carbon and total nitrogen analysis. The total inorganic carbon (TIC) was analysed using a coulometer (model CM 5015 CO_2, UIC Inc. USA). The pure limestone ($CaCO_3$) was used as standard, with carbon percentage of 12 %. The total carbon and total nitrogen content was analysed using the Flash 2000 series CN Elemental Analyzer. For total carbon and nitrogen analysis, NC Soil Standard was used. The nitrogen content in the standard was 0.21 ± 0.01 % and the carbon was 2.29 ± 0.07 %. The C_{org} was estimated by subtracting inorganic carbon from the total carbon. The $CaCO_3$ was estimated by multiplying the inorganic carbon by 8.33 (Johnson *et al.* 2014).

3.3. Radiocarbon dating

The radiocarbon dating provides the age of carbon-comprising material derived from the living organisms. The chronology of the top 1.5 m section of the core was established by five accelerator mass spectrometer (AMS) radiocarbon dates (Table 1). The surface-dwelling planktic foraminifera, namely *Globigerinoids ruber* and *Trilobatus sacculifer*, were picked for radiocarbon dating. The radiocarbon dates were obtained from the Inter University Accelerator Center, Delhi, India, and the Center for Applied Isotope Studies (CAIS) at the University of Georgia. The radiocarbon ages were calibrated using the CALIB 8.2 radiocarbon calibration program (Stuiver & Reimer, 1993; Reimer *et al.* 2013). A reservoir correction of 77 ± 58 yr from the nearby locations (Dutta *et al.* 2001; Southon *et al.* 2002) was used to calibrate the dates.

4. Results

4.1. Chronology

The chronology of the core was established by using the Bacon age model (Blaauw & Christen, 2011), utilizing the five AMS radiocarbon dates (Table 1; Fig. 3). Based on the sedimentation rate between the top two dated intervals (39.5 cm and 49.5 cm), the core top was assigned a modern age. The age of the bottommost section (149–150 cm) of the studied core was radiocarbon-dated to be 4600 ± 25 yr. The modelled age for the bottommost section is 4926 (−445 / +262) yr BP. The age uncertainty varies from a minimum of −46 / +100 yr towards the core top to −445 / +282 yr in the older section. Thus, the core

Table 1. AMS radiocarbon age details

Lab code	Sample interval (cm)	Depth (cm)	^{14}C age (yr BP)	^{14}C age error (±yr)	Calib. age range (yr BP)	Calib. age (kyr BP)
IUACD#20C3157	39–40	39.5	2163	34	1554 –1762	1.665
IUACD#20C3160	49–50	49.5	2529	36	2002 –2234	2.118
IUACD#20C3158	78–79	78.5	3025	34	2641 –2845	2.734
IUACD#20C3159	93–94	93.5	3964	33	3759 –3997	3.885
UGAMS#19794	149–150	149.5	4600	25	4612 –4823	4.713

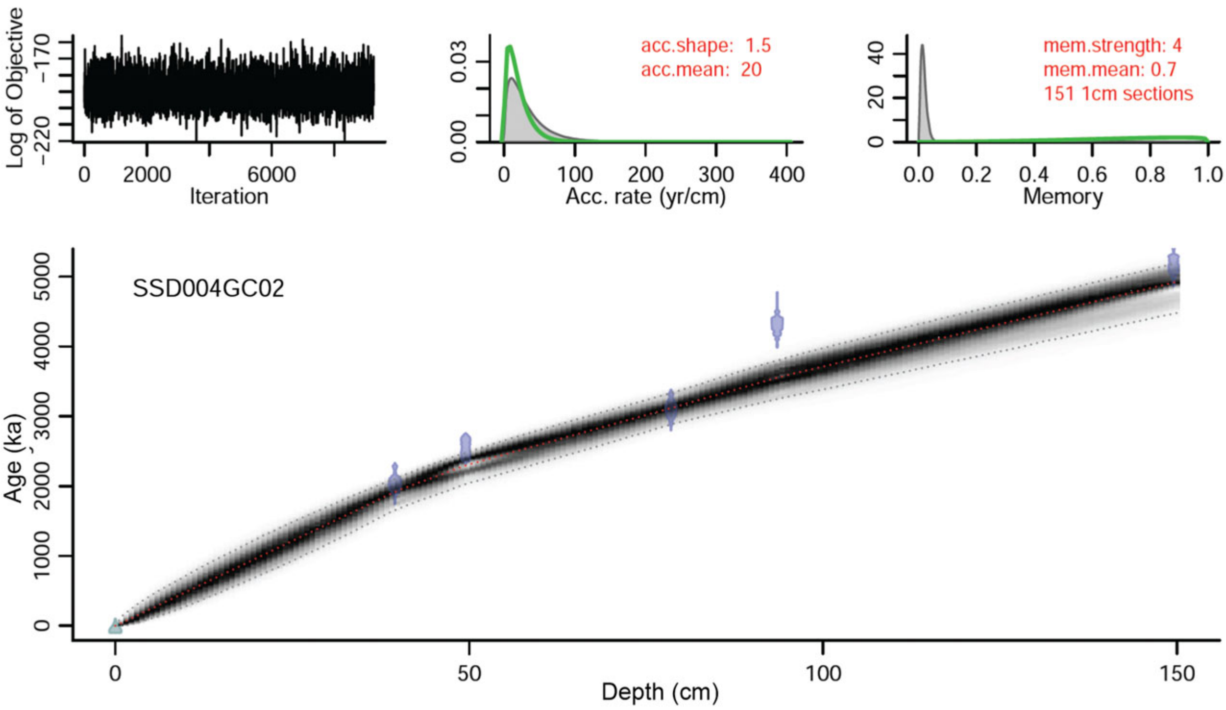

Fig. 3. (Colour online) The chronology of core SSD004 GC02 asestablished by Bacon age model, utilizing the AMS radiocarbon ages. The core top age was interpolated to be modern, based on the sedimentation rate between the subsequent radiocarbon-dated intervals. The radiocarbon ages are plotted as grey filled points, and the age uncertainty is marked by the dotted line envelope.

covers the entire Meghalayan Age. The sedimentation rate varied from 13.0 cm kyr^{-1} to 67.6 cm kyr^{-1}, with a mean sedimentation rate of 34.5 cm kyr^{-1} (Fig. 3). The sample resolution varied from 15 years to 77 years, with an average resolution of 41 years.

4.2. Coarse fraction (>63 μm)

The coarse fraction comprises of sand-sized sediments. As the sediments were not pre-treated, the sediments also contained biogenic carbonates. A gradual increase in coarse fraction abundance is observed from the bottom of the section to a depth of 90 cm (3.45 ka). The coarse fraction was most abundant (15.5 %) at 90 cm (3.45 ka). Subsequently, it decreased abruptly, only to increase again at 72 cm (2.93 ka). A very prominent abrupt decrease in coarse fraction (4.2 %) was observed at 47 cm (2.20 ka). The coarse fraction abundance increased again at 43 cm (2.05 ka). The coarse fraction decreased gradually from 43 cm onwards, except for a minor increase in the core top sections (Fig. 4).

4.3. Calcium carbonate ($CaCO_3$)

A 6 % decrease in $CaCO_3$ is observed from the bottom of the studied section up to a depth of 120 cm (4.20 ka) (Fig. 4). Subsequently, $CaCO_3$ increased rapidly up to a depth of 92 cm (3.51 ka). Later, the weight percentage of $CaCO_3$ decreased up to a depth of 78 cm (3.10 ka). From 3.08 ka onwards, $CaCO_3$ increased gradually up to a depth of 28 cm (1.36 ka) to reach a peak value of 35.0 %. Two prominent peaks, centred at 72 cm and 55 cm (2.91 ka and 2.45 ka, respectively), are observed within this gradual increase. The concentration of $CaCO_3$ remained uniform in the top ~25 cm section (1.17 kyr) of the core (Fig. 4).

4.4. Organic carbon (C_{org})

The down-core variation in C_{org} is similar to $CaCO_3$ (Fig. 4). A small decrease (0.3 %) in C_{org} is observed from the bottommost section until 4.39 ka (128 cm). The C_{org} gradually increased by 1.7 %, from 4.37 ka (127 cm) until 0.60 ka (15 cm). C_{org} remained

https://doi.org/10.1017/S001675682200111X Published online by Cambridge University Press

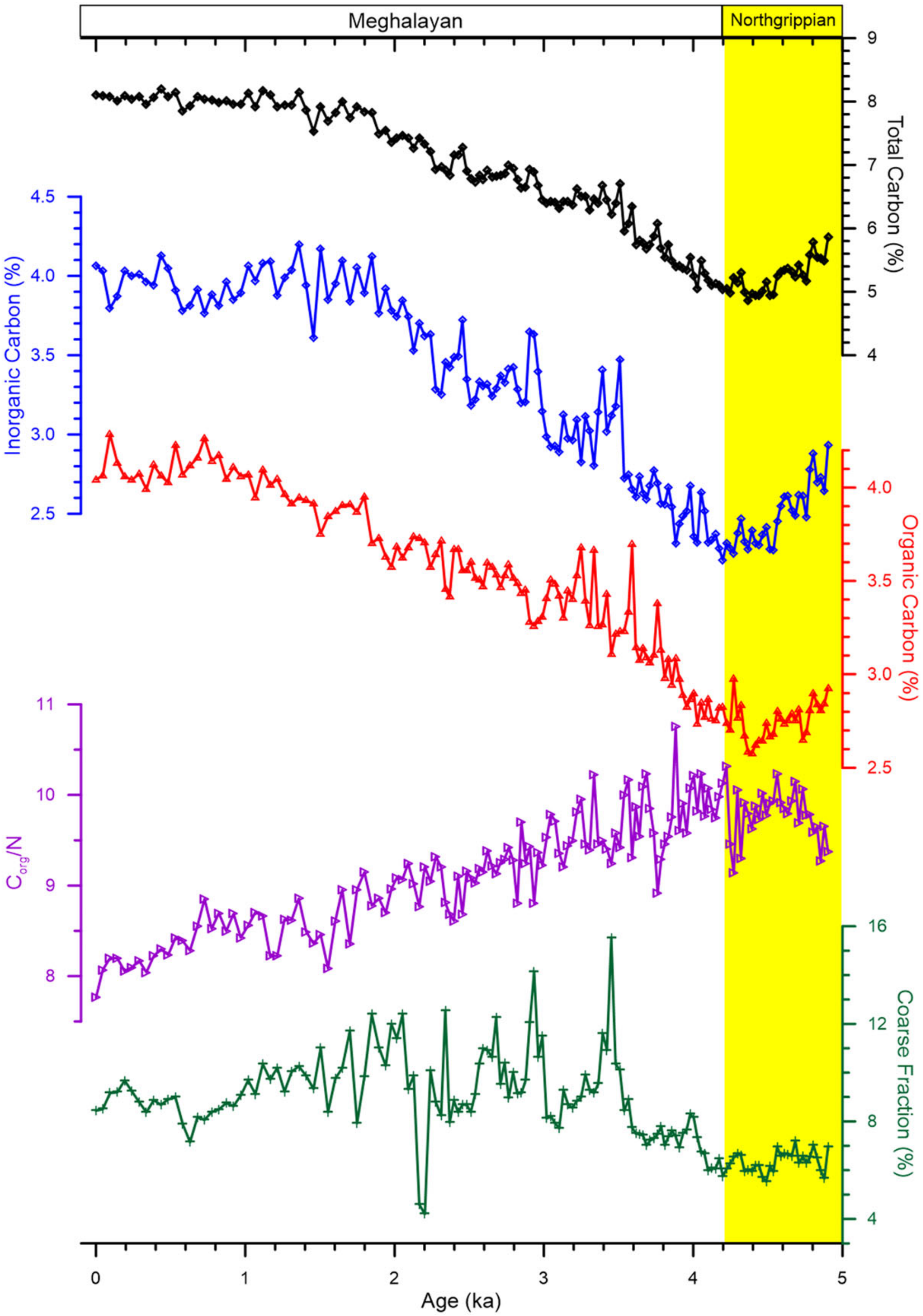

Fig. 4. (Colour online) Down-core variation in total carbon, inorganic carbon, organic carbon, C_{org}/N and coarse fraction (>63 μm) in core SSD004 GC02. The yellow shaded bar is the Northgrippian Age.

https://doi.org/10.1017/S001675682200111X Published online by Cambridge University Press

uniform in the top 15 cm section (0.68 kyr) of the core. A few minor variations are also observed within the gradual increase in C_{org}.

4.5. Organic carbon/nitrogen (C_{org}/N)

The organic matter in marine sediments accumulates from both the land and marine sources. The terrestrial and marine organic matter has a distinct carbon to nitrogen ratio (C_{org}/N) (Calvert *et al.* 1995) and thus is used to understand the change in the relative contribution of these two sources. C_{org}/N increased from the bottommost section until 4.51 ka (135 cm). A continuous decrease in C_{org}/N, from 10.56 to 7.76, is observed from 4.23 ka (122 cm) onwards to the core top (Fig. 4). Within this gradual decreasing pattern, a few prominent lows (4.02 ka, 102 cm and 1.36 ka, 32 cm) are also observed.

4.6. Planktic foraminiferal abundance (specimen/g sediment)

After a minor decrease from the bottommost section until 4.34 ka, the planktic foraminiferal abundance increased from 4.22 ka to 1.98 ka (~41 cm). Subsequently, the planktic foraminiferal abundance decreased until 0.25 ka (~7 cm). The abundance was again high in the top 7 cm section (0.29 kyr) of the core (Fig. 5). A few minor fluctuations in planktic foraminiferal abundance are also observed within the general trend stated above. The abundance varied from a minimum of 1945 specimen/g sediment at 4.22 ka (124.5 cm) to a maximum of 10 110 specimen/g sediment at 1.98 ka (41 cm).

4.7. Relative abundance of *Globigerina bulloides* (%)

Globigerina bulloides is a widely accepted upwelling indicator planktic foraminifer. The relative abundance of *G. bulloides* was low in the bottommost section of the core (average 18.0 % between 4.6 ka and 4.9 ka). The relative abundance increased and remained high (average 22.6 %) until 1.5 ka (32 cm). A prominent decrease in *G. bulloides* relative abundance was observed in the top 25 cm section (1.17 kyr) of the core (Fig. 5).

5. Discussion

The total carbon, $CaCO_3$ as well as C_{org}, was very low towards the end of the Northgrippian Age covered in the studied core section (4.2–4.9 ka) and the beginning of the Meghalayan Age. Following these low sedimentary carbon values at the Northgrippian–Meghalayan transition, both the organic and inorganic carbon increased throughout the Meghalayan Age. The beginning of the increase in C_{org} (4.4 ka) preceded that in $CaCO_3$ (4.2 ka) and resulted in higher total carbon burial in the Gulf of Mannar during the Meghalayan Age (Figs 6, 7). The low $CaCO_3$ as well as C_{org} during the Northgrippian–Meghalayan transition is attributed to weaker monsoon-induced productivity. The weaker summer monsoon at the Northgrippian–Meghalayan boundary has also been inferred from the terrestrial records (Enzel *et al.* 1999; Dixit *et al.* 2014; Kotlia *et al.* 2015). The persistent increase in total carbon, $CaCO_3$ as well as C_{org}, stabilized between 2.7 ka and 3.7 ka as well as in the top ~1.2 kyr section of the core.

In the SE Arabian Sea, $CaCO_3$ content in sediments is strongly coupled with monsoon (Guptha *et al.* 2005; Narayana *et al.* 2009). Thus, the increased C_{org}, $CaCO_3$ and nitrogen during the Holocene has often been used to infer higher productivity due to stronger summer monsoon in the eastern Arabian Sea (Kessarkar *et al.* 2010). A substantial fraction of the $CaCO_3$ is biogenic, comprising calcareous shells. Amongst a huge variety of calcareous marine organisms, foraminifera and coccolithophores contribute the largest fraction of the biogenic carbonate flux in the ocean (Ramaswamy & Gaye, 2006; Langer, 2008). The increase in $CaCO_3$ is thus mainly due to an increased abundance of foraminiferal shells. The diversity and abundance of foraminifera depends on the ambient conditions, especially food availability (Schiebel *et al.* 2001). In the northern Indian Ocean, monsoon influences the C_{org} flux, the food for foraminifera. Both summer and winter monsoons affect the primary productivity in the northern Indian Ocean by bringing nutrients from the land by terrigenous influx as well as through upwelling and convective mixing (Madhupratap *et al.* 1996; Sreeush *et al.* 2018). The enhanced terrigenous supply to the Arabian Sea and a subsequent increase in biological productivity during the summer monsoon has been confirmed by sediment trap studies (Nair *et al.* 1989). Many zooplanktons feeding on primary producers have a calcareous skeleton. The calcareous skeletons also sequester a substantial fraction of carbon and bury it in the ocean sediments. Thus the $CaCO_3$ in the sediments is influenced by productivity, dissolution of $CaCO_3$ and dilution by terrigenous material (Naidu, 1991; Pattan *et al.* 2019). The shift in monsoon-induced evaporation–precipitation during the Holocene was synchronous with a change in surface productivity, planktic foraminiferal abundance and coarse sediment fraction (Saraswat *et al.* 2016). In modern times, the higher primary productivity during the later phase of the summer monsoon is attributed to the coastal upwelling and river runoff bringing nutrients to the surface waters (Jyothibabu *et al.* 2008).

The increasing $CaCO_3$ thus suggests that the monsoon began to intensify at 4.0 ka, which would have enhanced the upwelling-induced productivity in the Gulf of Mannar (Naidu, 1991). The findings are in line with the records from the northern India and eastern Arabian Sea. Dixit *et al.* (2014) reported that the weak monsoon phase at the Northgrippian–Meghalayan transition lasted for only 200 years and further that the monsoon recovered to the present level by 4 ka. A clear monsoon intensification trend beginning at 4 ka is also observed in core 63KA recovered from the northern Arabian Sea (Staubwasser *et al.* 2003). A similar consistent increase in $CaCO_3$ in the SE Arabian Sea, during the late Holocene, was also attributed to the strengthened monsoon (Sarkar *et al.* 2000). The increasing trend in $CaCO_3$ in the Gulf of Mannar matches with another core (AAS-VI/GC-05) collected off Cochin from the SE Arabian Sea (Pattan *et al.* 2019), suggesting a strong regional feature (Fig. 7). However, the high primary productivity during the winter season could also drive the increase in $CaCO_3$. The increased Indus runoff during the late Holocene was attributed to strengthened winter monsoon precipitation (Staubwasser *et al.* 2003).

The higher primary productivity may not always result in increased biogenic carbonate flux. The bottom water conditions, including the dissolved oxygen concentration and grain size of the sediments, strongly influence the burial of both the C_{org} and biogenic carbonate. Incidentally, the increase in both the primary productivity and denitrification during the Northgrippian and Meghalayan (since ~7 ka) in the eastern Arabian Sea was reported to be coeval with an increase in $CaCO_3$ dissolution, as evident from the low $CaCO_3$ concomitant with low shell weight and prominent dissolution features in the shells, suggesting a significant regional bias in preservation (Naik *et al.* 2014). The decreased $CaCO_3$ was contemporaneous with the lowest dissolved oxygen levels in the bottom waters (Naik *et al.* 2014). Thus, the preservation of

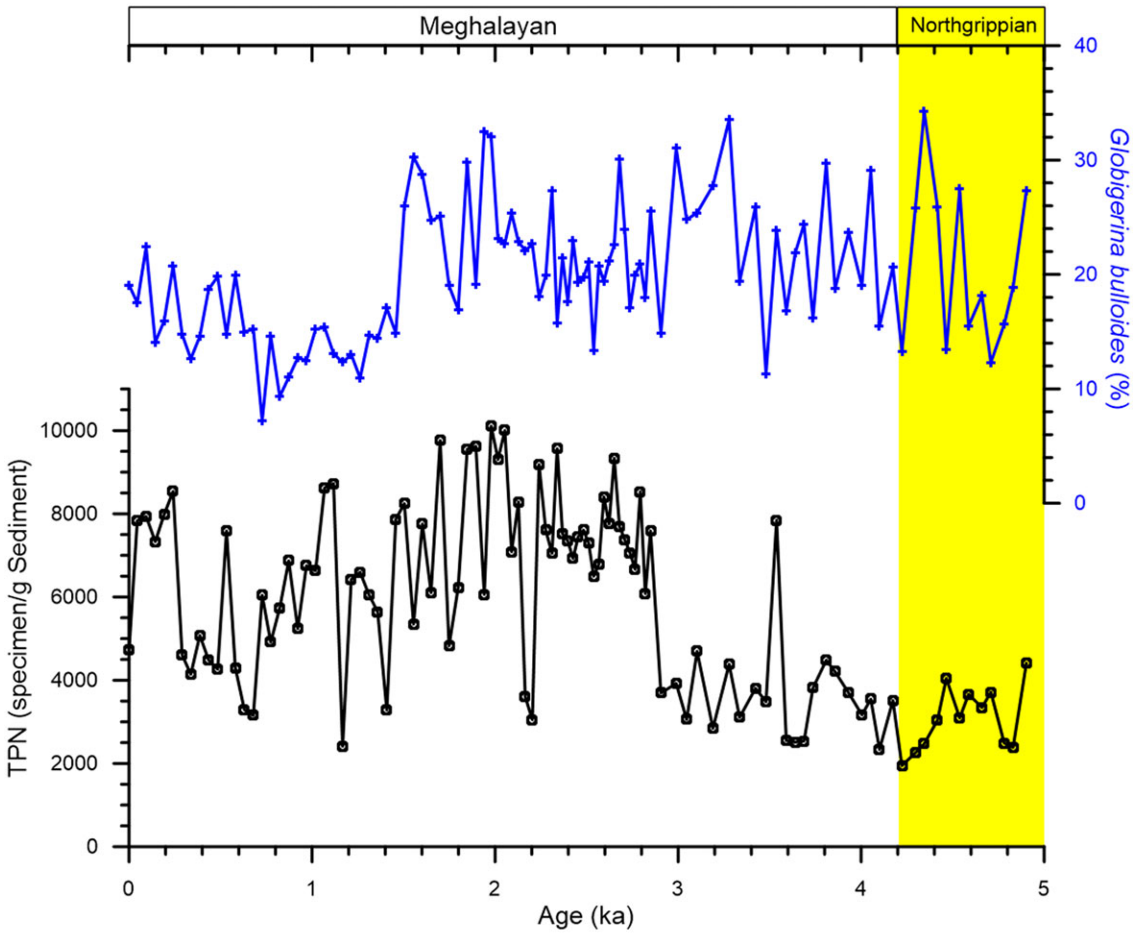

Fig. 5. (Colour online) The absolute abundance of planktic foraminifera normalized to 1 g dry sediment and the relative abundance of upwelling indicator species *Globigerina bulloides* in core SSD004 GC02. The yellow shaded bar is the Northgrippian Age.

foraminiferal carbonate in the ocean sediments resulting in long-term carbon burial, varies regionally (Naik *et al.* 2017) and depends on sedimentation rate (Agnihotri *et al.* 2003*b*) and bottom water conditions (pH, $CaCO_3$ compensation depth). Earlier, similar higher productivity and extreme suboxic condition during the late Holocene (5.5 ka to present) were reported from the SE Arabian Sea (Pattan *et al.* 2019). Therefore, the consistent increase in $CaCO_3$ in the Gulf of Mannar suggests persistence of conditions favouring carbon burial in the sediments. The stabilization of carbon burial in the Gulf of Mannar in the last 1.5 kyr suggests weakening of the upwelling during the summer monsoon, as also inferred from the terrestrial records (Sanwal *et al.* 2013). The weakened upwelling signature in the Gulf of Mannar during the last 1.5 kyr is, however, opposite to that of the western Arabian Sea (Gupta *et al.* 2003). The response of this region to summer monsoon winds is different than that of the western Arabian Sea (Bassinot *et al.* 2011). It should, however, be noted here that the carbon burial in the upper section of the core might also be influenced by anthropogenic activities.

5.1. Organic carbon (C_{org}) contribution

The C_{org} increased throughout the Meghalayan Age, with the exception of the interval between 2.7 ka and 3.7 ka, as well as the top 1.2 kyr section (Fig. 6). A few other records from the SE Arabian Sea also have an increasing C_{org} burial during the Meghalayan Age, suggesting increased productivity mainly controlled by the summer monsoon (Diniz *et al.* 2018). A similar progressive increase in productivity is observed in the SE Arabian Sea, throughout the Holocene, with a sharp jump at 5.4 ka (Naik *et al.* 2017). The increase in C_{org} in the SE Arabian Sea since the mid-Holocene has been attributed to better preservation facilitated by the higher sedimentation rate and reducing conditions (Nagoji & Tiwari, 2017). The principal reason for the increased C_{org} accumulation in the sediments is the organic matter flux from the highly productive surface waters. Both, the strong upwelling due to intense summer monsoon (Sarma *et al.* 2007) and convective mixing during the winter season (Madhupratap *et al.* 1996) increase the primary productivity and the subsequent organic matter flux. Thus, a strong monsoon leads to an increase in productivity and subsequent higher C_{org} flux to the seafloor (Sreeush *et al.* 2018). The strong influence of monsoon on the biological productivity in the Arabian Sea has been confirmed from the sediment trap studies. The biological productivity is generally high during the summer monsoon (Nair *et al.* 1989). Additionally, increased productivity, lower than that during the summer season but higher than that in the non-monsoon months, is observed during the winter season (Nair *et al.* 1989; Guptha *et al.* 1997). The past records also demonstrate a strong influence of productivity on organic matter flux. A substantial increase in C_{org} content and $CaCO_3$ in the eastern Arabian Sea has been reported during the Holocene, and attributed to the increased productivity

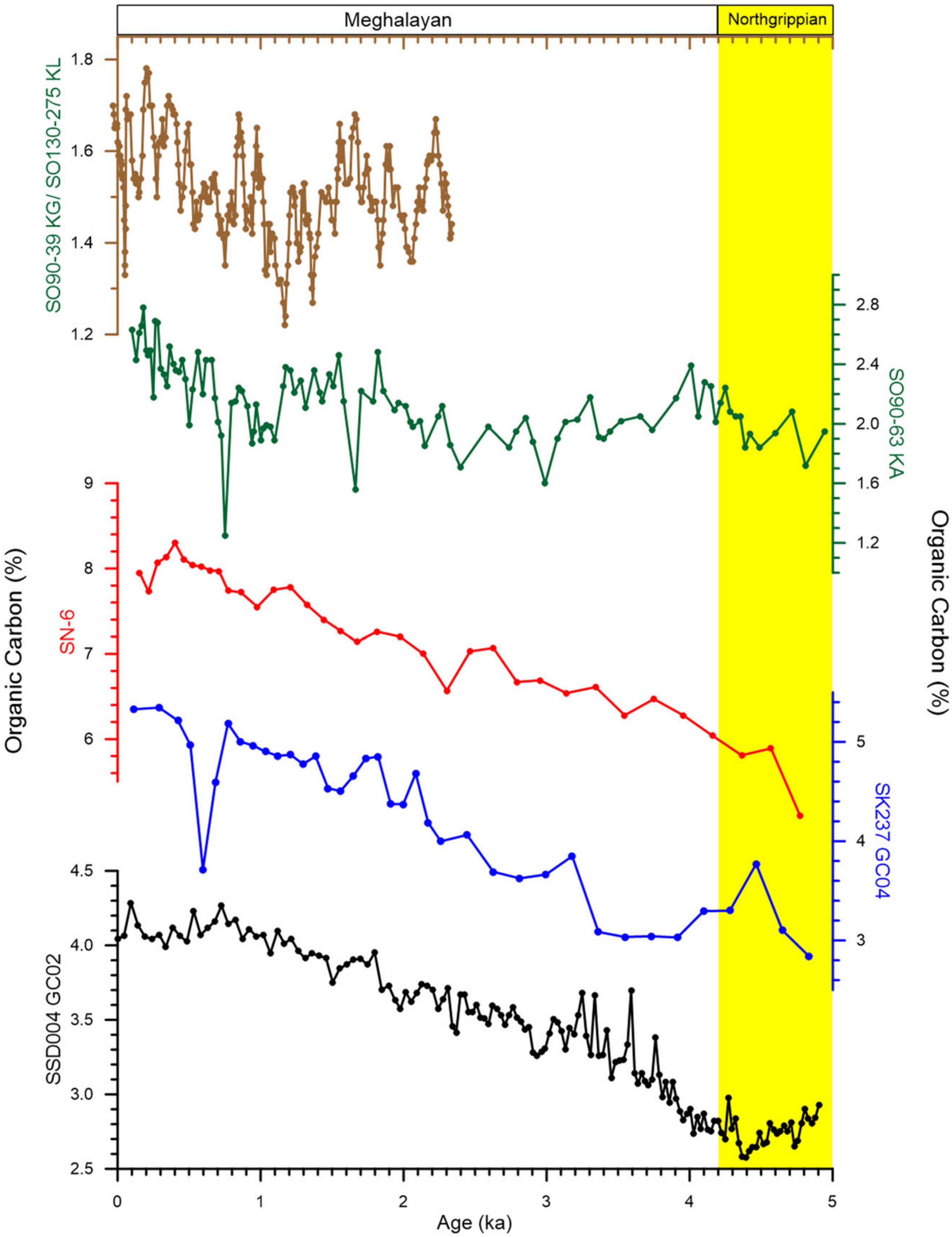

Fig. 6. (Colour online) A comparison of C_{org} variation in the Gulf of Mannar (SSD004 GC02) during the last 5 kyr with that in different parts of the eastern Arabian Sea (SO90-39 KG/SO130-275 KL, Böll *et al.* 2014; SO90-63 KA, Burdanowitz *et al.* 2019; SK291 GC15, Saravanan *et al.* 2019; SN-6, Nagoji & Tiwari, 2017; SK237 GC04, Naik *et al.* 2017). The yellow shaded bar is the Northgrippian Age.

https://doi.org/10.1017/S001675682200111X Published online by Cambridge University Press

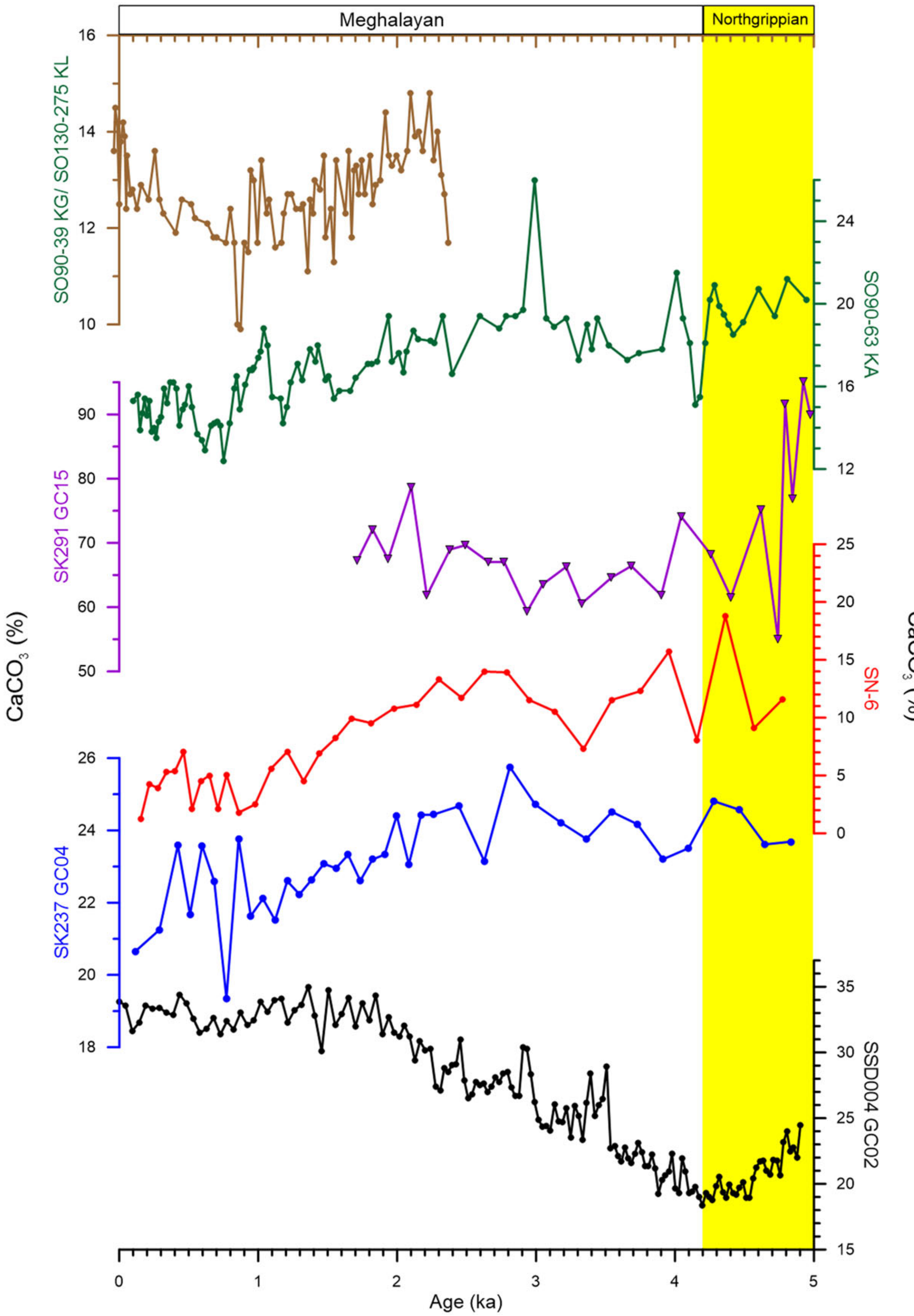

Fig. 7. (Colour online) A comparison of $CaCO_3$ wt % variation in the Gulf of Mannar (SSD004 GC02) during the last 5 kyr with that in different parts of the eastern Arabian Sea (SO90-39 KG/SO130-275 KL, Böll *et al.* 2014; SO90-63 KA, Burdanowitz *et al.* 2019; SK291 GC15, Saravanan *et al.* 2019; SN-6, Nagoji & Tiwari, 2017; SK237 GC04, Naik *et al.* 2017). The yellow shaded bar is the Northgrippian Age.

(Thamban *et al.* 1997; Agnihotri *et al.* 2003*a*). Thus the increased C_{org} accumulation during most of the Meghalayan Age in the Gulf of Mannar can be attributed to increased productivity. However, it is to be noted that the quick burial and dissolved oxygen concentration at the sediment–water interface strongly modulate C_{org} preservation.

The core is located towards the lower boundary of the oxygen minimum zone. Therefore, the temporal variation in carbon burial is likely to be influenced by the changes in bottom water oxygen concentration. In the eastern Arabian Sea, the higher C_{org} concentration coincides with the oxygen minimum zone (OMZ; 150–1500 m), suggesting the strong influence of anoxic bottom waters in preserving the organic matter (Paropkari *et al.* 1992). However, from the subsequent studies covering a broader zone, it was found that the C_{org} and nitrogen are maximum between 200 and 1600 m depth and the lowest dissolved oxygen is at 200 and 800 m depth (Calvert *et al.* 1995). Thus, although the deficient oxygen is one of the factors favouring better organic matter preservation, variation in supply, dilution by other sedimentary components and texture of the sediment also strongly influence the amount of organic matter buried in the sediments (Calvert *et al.* 1995). The C_{org} and $CaCO_3$ show a similar trend throughout the core, except for a few minor short-term deviations (between 2.6 ka and 3.6 ka). The $CaCO_3$ fraction in the sediment decreased whereas C_{org} increased from 3.0 ka to 3.4 ka. The subsequent abrupt increase in the $CaCO_3$ fraction at 2.9 ka was contemporaneous with a decrease in C_{org}. The short-term opposite trend of C_{org} and $CaCO_3$ concentration is due to diagenetic effects, mainly sulphate reduction and other associated processes. The sulphate reduction dissolves the $CaCO_3$, but a higher sedimentation rate and increased clay content lead to a better preservation of C_{org} (Bhushan *et al.* 2001).

5.2. Upwelling indicator planktic foraminifera

The relative abundance of *G. bulloides* was higher than average (20.0 %), between 4.50 ka and 1.50 ka and lower in the last 1.47 kyr. A few planktic foraminifera thrive in upwelled colder, nutrient-rich waters with plenty of food. *Globigerina bulloides* is one such planktic foraminifera species abundant in cold, organic-matter-rich waters and thus is used as an indicator of upwelling (Auras-Schudnagies *et al.* 1989; Saraswat & Khare, 2010; Naik *et al.* 2017). From the foraminiferal distribution during the summer monsoon, it was suggested that the change in the relative abundance of *G. bulloides* could be used to trace the palaeo-upwelling intensity (Prell & Curry, 1981) and thus the associated summer monsoon strength and productivity in both the Arabian Sea and Bay of Bengal (Naidu *et al.* 1999). The relative abundance of *G. bulloides* in the Gulf of Mannar is comparable with that in typical summer-monsoon-wind-induced upwelling-affected regions like the western Arabian Sea (Gupta *et al.* 2003). Therefore, the higher relative abundance of *G. bulloides* between 1.50 ka and 4.50 ka (average 22.6 %) suggests intense upwelling and thus strengthened summer monsoon during the larger part of the Meghalayan Age, as compared to the last 1.5 kyr (Fig. 8). The change in the relative abundance of *G. bulloides* in the Gulf of Mannar is, however, different than that in the western Arabian Sea (Gupta *et al.* 2003; Saravanan *et al.* 2019). The abundance consistently decreases in the western Arabian Sea from ~5 ka until ~1.5 ka (Gupta *et al.* 2003), whereas we see a higher relative abundance of *G. bulloides* between 1.50 ka and 4.50 ka, but no consistent increasing or decreasing trend. The difference is attributed to the varying response of the different parts of the Indian Ocean to the summer-wind-intensity and direction-induced upwelling (Bassinot *et al.* 2011). The change in the relative abundance of *G. bulloides* between 1.5 ka and 4.5 ka slightly matches with that in a core (SK291/GC15) collected from the central eastern Arabian Sea (Saravanan *et al.* 2019). However, we need to mention that core SK291/GC15 was collected from a very weak upwelling area (Saravanan *et al.* 2019). A similar higher *G. bullodies* during most of the Meghalayan Age was also reported in another core (MD77-191) collected from the nearby SE Arabian Sea (Bassinot *et al.* 2011). The last ~1.5 kyr record is missing from MD77-191, hampering the comparison of our late Meghalayan Age record with this core.

It is interesting to note that although the relative abundance of *G. bulloides* was consistently high during the early Meghalayan Age, we did not see any persistent increasing trend. The lack of any increasing trend in *G. bulloides* relative abundance suggests additional factors facilitating increased productivity and thus C_{org} flux. It is likely that the increased carbon burial was due to the increased productivity during the winter season coupled with better preservation. The Gulf of Mannar receives precipitation during the winter season. The rivers debouching in the Gulf of Mannar bring nutrient-rich turbid waters during the winter season (Chandramohan *et al.* 2001). Additionally, the nutrient-rich water advects from the Palk Bay, in the SW Bay of Bengal, to the Gulf of Mannar (Jyothibabu *et al.* 2021). Therefore, the zooplankton biomass and chlorophyll-*a* concentration is high during both the summer and winter monsoon seasons in the Gulf of Mannar, suggesting increased productivity (Jagadeesan *et al.* 2013). The nearly fourfold increase in planktic foraminifera abundance from 1945 specimen/g sediment at 4.22 ka to 10110 specimen/g sediment at 1.98 ka suggests an overall increase in productivity, during this interval. As the summer-monsoon-induced upwelling, although it was high, did not increase consistently, the increase in productivity between 4.22 ka and 1.98 ka, as inferred from planktic foraminifera abundance, is attributed to intense winter monsoon.

On the finer timescale, from the relative abundance of *G. bulloides,* we report a weaker monsoon between 2.65 ka and 2.28 ka and a subsequent strengthening of the monsoon between 2.05 ka and 1.50 ka. The weak monsoon followed by the strengthened monsoon phase between 2.05 ka and 1.50 ka in the Gulf of Mannar core is similar to the weakening of the monsoon at 2 ka and the subsequent wet phase, inferred from the eastern Arabian Sea (Khare *et al.* 2008). However, the duration of the wet phase in the two records is different, likely because the region off Goa is mainly influenced by the summer monsoon, while the Gulf of Mannar receives substantial precipitation during both the summer and winter seasons. A part of the difference may also be because of the different radiocarbon age calibration methods followed in these records. The decreased *G. bulloides* abundance during the last 1 kyr, however, suggests a weakened summer monsoon. The impact of weakened summer monsoon during the last 1 kyr is evident in deceased C_{org} and $CaCO_3$ accumulation in the Gulf of Mannar. However, the Gupta *et al.* (2003) *G. bulloides* percentage data would suggest an increase in upwelling and thus strengthened summer monsoon winds during the last 1 kyr. The different trend in *G. bulloides* in the Gulf of Mannar and the western Arabian Sea is attributed to the differential response of these two regions to the summer winds (Bassinot *et al.* 2011).

https://doi.org/10.1017/S001675682200111X Published online by Cambridge University Press

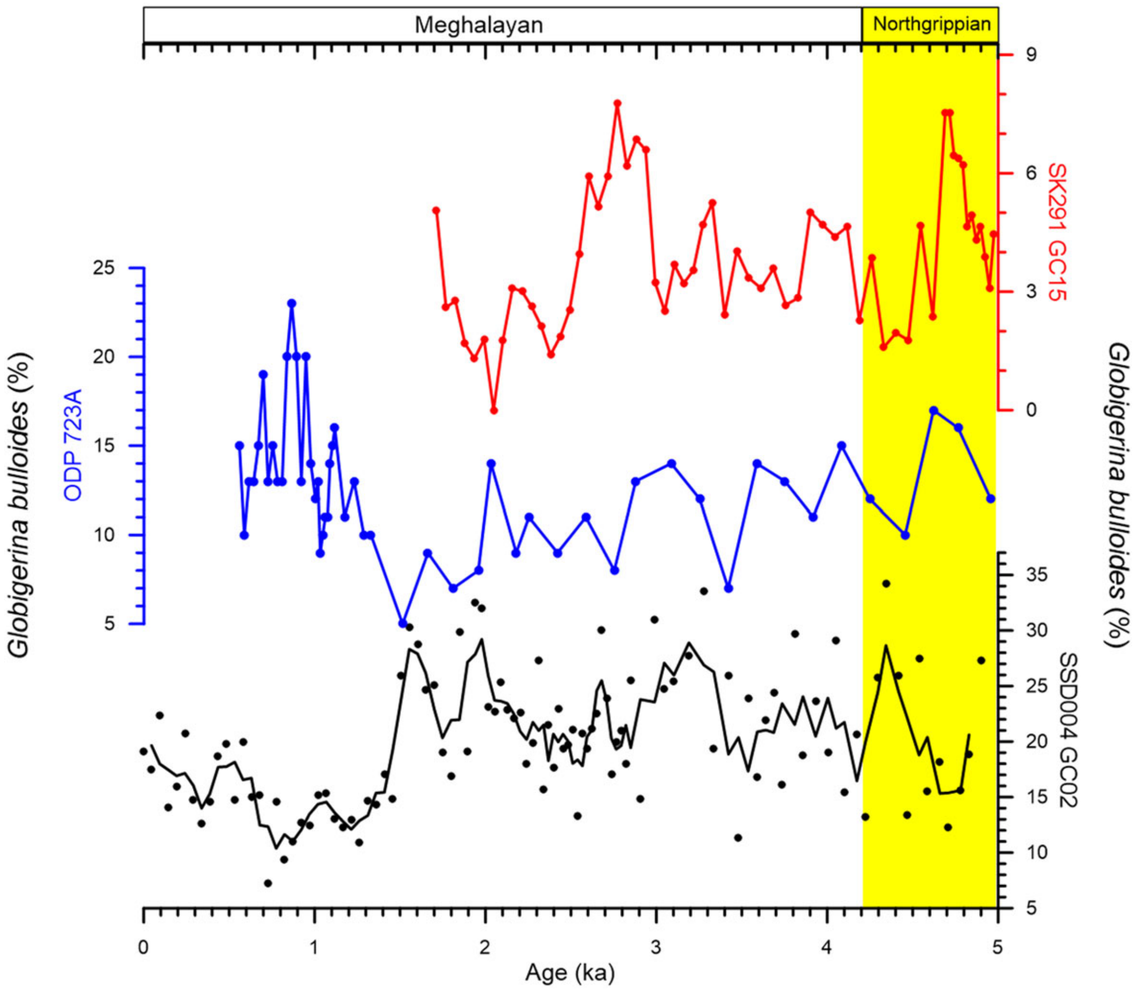

Fig. 8. (Colour online) The relative abundance of monsoon wind forced upwelling-induced cold nutrient-rich water indicator *Globigerina bulloides* in the Gulf of Mannar (SSD004 GC02), Oman Margin (ODP 723A, Gupta *et al.* 2003) and central eastern Arabian Sea (SK291 GC15, Saravanan *et al.* 2019). The yellow shaded bar is the Northgrippian Age.

5.3. Terrestrial versus marine organic carbon contribution

The C_{org}/N increased during the Northgrippian but consistently decreased from 4.0 ka onwards until recent times. Although, the overall decrease in C_{org}/N during the Meghalayan Age was ~2, the trend was very prominent. In addition to the primary productivity, a substantial fraction of the organic matter in the ocean, especially the marginal marine regions, is also of terrestrial origin, brought by the river runoff as well as winds. The marine and terrestrial contribution of the organic matter is delineated with the help of C_{org}/N (Calvert *et al.* 1995). The marine organic matter has a relatively lower C_{org} to nitrogen ratio as compared to terrestrial plants. The C_{org}/N ratio is thus an index to determine the relative contribution of marine or terrestrial organic matter. The terrigenous organic matter generally has a high C_{org}/N (>20), whereas marine origin organic matter has low C_{org}/N (5–8) (Jasper & Gagosian, 1989). The C_{org} in core SSD004 GC02 is increasingly of marine origin, based on C_{org}/N ratio (Fig. 9). The gradually decreasing C_{org}/N ratio throughout the core confirms the increase in marine organic matter contribution to the C_{org} throughout the Meghalayan Age. The decreasing terrestrial organic matter contribution is attributed to the increasing distance of the core site from the Thamirabarani River due to a >10 m rise in sea-level since the beginning of the Meghalayan Age (Grant *et al.* 2014), as well as the increase in marine productivity. The increasing marine contribution to the organic matter, despite there being no such trend in upwelling indicator *G. bulloides*, further supports our inference of higher primary productivity due to winter monsoon in the Gulf of Mannar.

5.4. Comparison with regional high-resolution records

We compared the SSD004 GC02 $CaCO_3$ and C_{org} with other similar high-resolution records from the eastern Arabian Sea (SO90-39 KG/SO130-275 KL, Böll *et al.* 2014; SO90-63 KA, Burdanowitz *et al.* 2019; SN-6, Nagoji & Tiwari, 2017; SK237 GC04, Naik *et al.* 2017). All these records are from the continental slope region. A couple of these records (SO90-39 KG/SO130-275 KL and SO90-63 KA) are from the NE Arabian Sea. The primary productivity is very high in the NE Arabian Sea due to convective mixing during the winter (Madhupratap *et al.* 1996) and advection of high-nutrient water from the western Arabian Sea during the summer (Saraswat *et al.* 2020). A similar high productivity during both the summer and winter seasons is also observed in the Gulf of Mannar, although the physical mechanisms are different than those in the NE Arabian Sea. A large difference is observed in both the trend and absolute abundance of $CaCO_3$ during the last 5 kyr in these

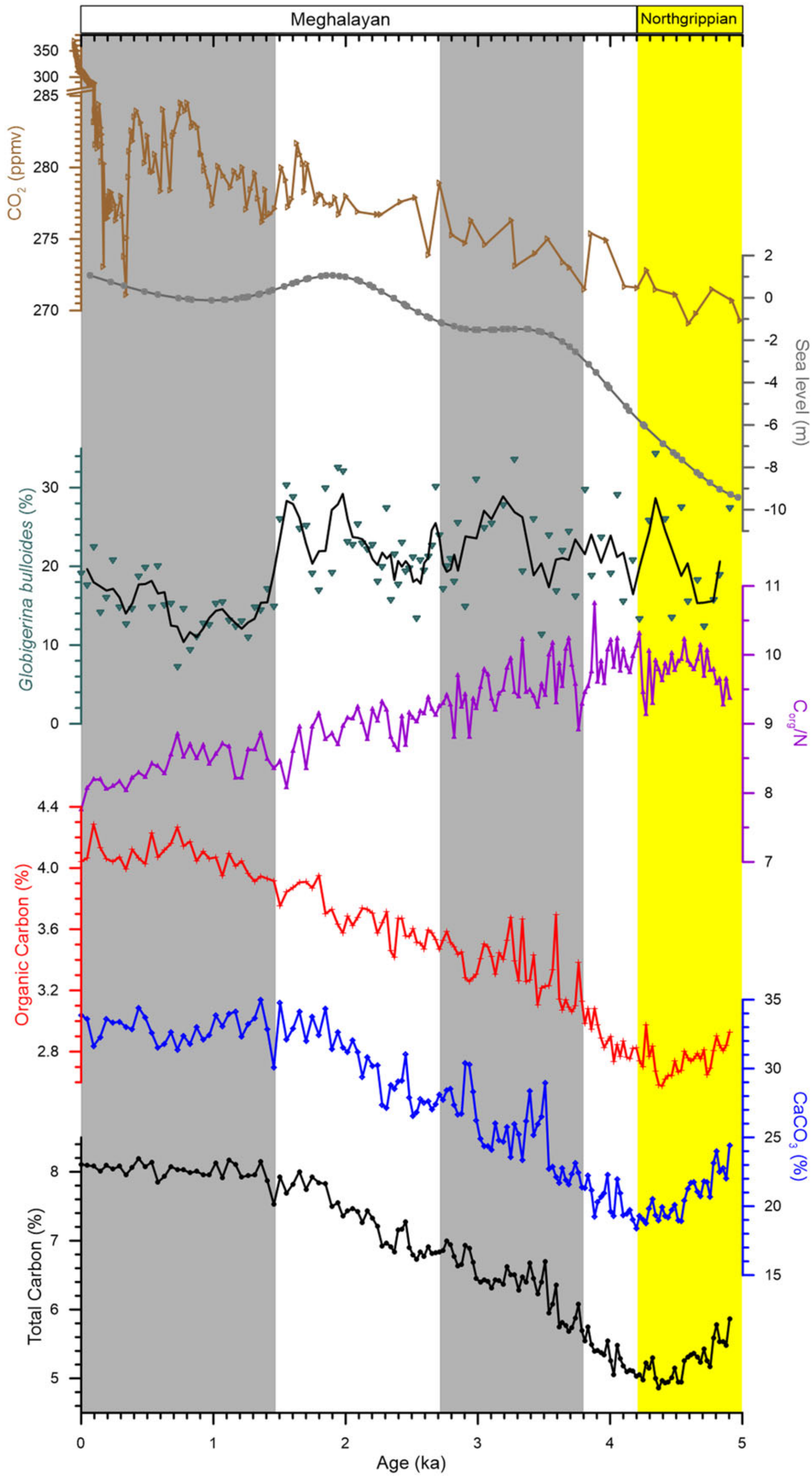

Fig. 9. (Colour online) The change in total carbon, $CaCO_3$, C_{org}, C_{org}/N and relative abundance of *Globigerina bulloides* during the Meghalayan Age, compared with the sea-level changes (Grant *et al.* 2014) and atmospheric CO_2 concentration (Bereiter *et al.* 2015). The yellow shaded bar is the Northgrippian Age. The intervals of significant change are marked by grey shaded regions.

two regions (Fig. 7). The Gulf of Mannar $CaCO_3$ record is different than other SE Arabian Sea records (Nagoji & Tiwari, 2017, Naik *et al.* 2017), but strikingly similar to another core, AAS-VI/GC-05, collected from a depth of 280 m in the SE Arabian Sea (Pattan *et al.* 2019). The SE Arabian Sea is influenced by upwelling-induced primary productivity during the summer season.

https://doi.org/10.1017/S001675682200111X Published online by Cambridge University Press

Amongst these regions, the highest $CaCO_3$ was in the Gulf of Mannar during the Meghalayan Age. We report a significant increase in $CaCO_3$ between ~1 ka and 3 ka, as compared to a consistent decrease in several other records. The records, however, match in a constant $CaCO_3$ during the last millennium. Interestingly, C_{org} consistently increased throughout the Meghalayan Age in all the records (Fig. 6). A similar C_{org} but different $CaCO_3$ in various parts of the eastern Arabian Sea is intriguing. A relatively high $CaCO_3$ in the Gulf of Mannar is attributed to its better preservation, due to a less intense oxygen-deficient zone as compared to the NE Arabian Sea (Sarma *et al.* 2020). The increased microbial respiration in a C_{org}-rich environment decreases the pH, leading to dissolution of biogenic carbonates (Cai *et al.* 2011). A similar C_{org} in all records suggests comparable productivity as well as its burial in sediments throughout the eastern Arabian Sea.

5.5. Factors affecting carbon burial and preservation

The preservation of both the biogenic $CaCO_3$ and organic matter in the sediments depends on ambient conditions. One of the major factors influencing organic matter preservation is the grain size. The finer grains preserve more organic matter (Bergamaschi *et al.* 1997). The sediments in the oceans are mainly brought by rivers or wind. The distance of a marine region from the river mouth thus affects the size and volume of the sediments being brought into an area. The sea-level also controls the grain size. The transgressing sea-level inundates and the regressing sea-level exposes the continental shelf. In the case of the marine regions close to the river mouth, the change in sea-level significantly shifts the point of sediment debouchment by rivers (Phillips & Slattery, 2006). Therefore, sea-level changes significantly affect the size as well as the volume of sediments being brought into the marginal marine regions and deeper waters through channels, and thus affect the carbon burial in marine sediments. The terrigenous dilution and/or dissolution increases the amplitude of the carbonate cycle but reduces $CaCO_3$ concentration in the Indian Ocean (Olausson, 1971; Naidu, 1991). The sea-level has increased by >10 m since the beginning of the Meghalayan Age (Grant *et al.* 2014; Fig. 9). The transgressing sea-level completely inundated the extensive, gently sloping relict carbonate platform along the southern margin of India (Hashimi *et al.* 1982). A significantly consistent $CaCO_3$ between 2.7 ka and 3.7 ka, matches with a decreased rate of sea-level rise during the same interval, as against a comparatively rapid rate of sea-level increase in the early Meghalayan Age. The inundation of the carbonate platform thus increased the distance of the core site from the nearby Thamirabarani River and thus reduced the coarse fraction supply to the area. However, the quantity and grain size of the sediments supplied by the river to the core site can also change due to the delta lobe avulsion as it is closely linked with the sea-level change (Chadwick & Lamb, 2021). The substantial change in terrigenous fraction and $CaCO_3$ was also highlighted from the western margin of India (Khare, 2018). In the SE Arabian Sea, the change in C_{org} during the glacial–interglacial interval was attributed to the variation in sediment texture as a result of higher terrigenous supply leading to increased dilution (Narayana *et al.* 2009). The resultant increase in finer fraction facilitated better preservation of both the organic matter and the biogenic carbonate.

The seawater pH at the sediment–water interface as well as of the pore water, also strongly modulates carbon burial (Keil, 2017; LaRowe *et al.* 2020; Freitas *et al.* 2022). As the core site lies in the oxygen-deficient zone, the pH at the sediment–water interface is likely to strongly modulate carbon burial in the sediments, before the remineralization of both the organic matter and $CaCO_3$. All such factors also have to be evaluated to fully understand the temporal changes in carbon burial in this region. With the available data, it is clear that both the intense monsoon-induced primary productivity and increasing sea-level facilitated the persistent increase in both the inorganic and carbon burial in the Gulf of Mannar, throughout the Meghalayan Age. However, the uniform carbon concentration in the topmost section of the core is most likely influenced by anthropogenic activities.

5.6. Carbon burial during the last millennium

A distinct shift in almost all the parameters in the top ~25 cm section representing the last ~1.17 kyr is intriguing. We want to state that this section has a chronological uncertainty as the age of the top section of the core was interpolated based on the sedimentation rate between the subsequent radiocarbon-dated intervals (39.5 cm and 49.5 cm). The total carbon remains uniform in this section, mainly due to the similar trend in $CaCO_3$. The increasing trend in C_{org} also flattens in the top ~15 cm section of the core. The atmospheric CO_2 concentration increased rapidly during the later part of this interval, driven by increased fossil fuel usage since the beginning of the industrial revolution (Fig. 9; Bereiter *et al.* 2015). The low relative abundance of *G. bulloides* in this section suggests a reduced upwelling and thus weaker summer monsoon. A weaker summer monsoon during the Late Meghalayan Age has also been reported from the terrestrial records (Srivastava *et al.* 2017). Thus the flattening of the total carbon burial during the last 1.17 kyr was driven by the weakening of the summer monsoon. It should, however, be noted here that the findings are in contrast with the high relative abundance of *G. bulloides* during the similar interval in the western Arabian Sea, suggesting a stronger monsoon-induced upwelling (Gupta *et al.* 2003). The differential response of these two regions is attributed to the difference in the orientation of the coastline to the wind direction and thus upwelling (Bassinot *et al.* 2003). Thus, it is clear that the summer-winds-driven upwelling-induced productivity decreased during the last 1.17 kyr in the Gulf of Mannar.

5.7. Implications for carbon cycling

The increase in carbon burial during the Meghalayan Age in the eastern Arabian Sea coincides with ~10 ppmv increase in the global atmospheric CO_2 (Fig. 9; Bereiter *et al.* 2015). It is intriguing that the atmospheric CO_2 increased during times of enhanced carbon burial. The opposite trend between the atmospheric CO_2 and carbon burial in the eastern Arabian Sea can be explained by several factors. First and the foremost is the regional nature of the carbon burial, with the ambient conditions in the Gulf of Mannar being favourable for carbon burial during the Meghalayan Age. Another factor contributing CO_2 is the carbonate counter pump, whereby precipitation of $CaCO_3$ by the marine organisms increases the CO_2 concentration in the surface waters and its subsequent efflux to the atmosphere (Salter *et al.* 2014). The increase in planktic foraminifera abundance during the early Meghalayan Age must have contributed CO_2 to the surface waters and subsequently to the increasing atmospheric CO_2, through the carbonate counter pump.

6. Conclusions

We report a persistent increase in the total carbon, $CaCO_3$ and C_{org} in the Gulf of Mannar, throughout the Meghalayan Age, except the bottommost (4.9 ka to 4.2 ka, 120–150 cm) and the topmost section (1.17 kyr, 0–25 cm) of the core. The increase in $CaCO_3$ and C_{org} is concomitant with a phase of high relative abundance of the upwelling indicator *G. bulloides* in the early Meghalayan Age, suggesting intense upwelling in response to the strong monsoon. The increasing planktic foraminifera abundance and decreasing C_{org}/N ratio suggest higher marine productivity due to winter monsoon. Thus the high $CaCO_3$ and C_{org} content in the Gulf of Mannar during most of the Meghalayan Age is attributed to high primary productivity influenced by the consistent summer and strong winter monsoon. The corresponding increase in sea-level during the early phase of the Meghalayan Age facilitated better preservation of both the C_{org} and $CaCO_3$, thus leading to increased carbon burial in the SE Arabian Sea. The uniform carbon content in the top section of the core is attributed to the weakening of the summer monsoon.

Acknowledgements. Authors acknowledge the help by Dr C Prakash Babu and Ms Teja Naik in analysing the total and inorganic carbon, using the Central Analytical Facility of the CSIR–National Institute of Oceanography. We thank Dr Dharmendra Pratap Singh, Assistant Professor, Indian Institute of Technology, Roorkee, for the Bacon age model based chronology of the core. Authors also acknowledge the help by Shri Shashikant Velip in collecting the core samples during the cruise. RS is grateful for financial support by the Science and Engineering Research Board, Department of Science and Technology, Government of India (CRG/2019/000221), and the Council of Scientific and Industrial Research in the form of Young Scientist project. Authors thank the technical staff at the radiocarbon-dating facility of the Inter-University Accelerator Center, India. We also thank Prof. Peter Clift, Editor, *Geological Magazine*, Dr Zhaokai Xu, Key Laboratory of Marine Geology and Environment, Institute of Oceanology, Chinese Academy of Sciences, China, and an anonymous reviewer for comments and suggestions to improve the manuscript. This is National Institute of Oceanography, Goa, India contribution number 6980.

References

Agnihotri R, Bhattacharya SK, Sarin MM and Somayajulu BLK (2003a) Changes in surface productivity and subsurface denitrification during the Holocene: a multiproxy study from the eastern Arabian Sea. *The Holocene* **13**, 701–13.

Agnihotri R, Sarin MM, Somayajulu BLK, Jull AT and Burr GS (2003b) Late-Quaternary biogenic productivity and organic carbon deposition in the eastern Arabian Sea. *Palaeogeography, Palaeoclimatology, Palaeoecology* **197**, 43–60.

Auras-Schudnagies A, Kroon D, Ganssen GM, Hemleben C, Van Hinte JE (1989) Biogeographic evidence from planktic foraminifers and pteropods for Red Sea anti-monsoonal surface currents. *Deep-Sea Research* **10**, 1515–33.

Azharuddin S, Govil P, Singh AD, Mishra R, Agrawal S, Tiwari AK and Kumar K (2017) Monsoon-influenced variations in productivity and lithogenic flux along offshore Saurashtra, NE Arabian Sea during the Holocene and Younger Dryas: a multi-proxy approach. *Palaeogeography, Palaeoclimatology, Palaeoecology* **483**, 136–46.

Bassinot FC, Marzin C, Braconnot P, Marti O, Mathien-Blard E, Lombard F and Bopp L (2011) Holocene evolution of summer winds and marine productivity in the tropical Indian Ocean in response to insolation forcing: data-model comparison. *Climate of the Past* **7**, 815–29.

Bereiter B, Eggleston S, Schmitt J, Nehrbass-Ahles C, Stocker TF, Fischer H, Kipfstuhl S and Chappellaz J (2015) Revision of the EPICA Dome C CO_2 record from 800 to 600 kyr before present. *Geophysical Research Letters* **42**, 542–9. doi: 10.1002/2014GL061957.

Bergamaschi BA, Tsamakis E, Keil RG, Eglinton TI, Montluçon DB and Hedges JI (1997) The effect of grain size and surface area on organic matter, lignin and carbohydrate concentration, and molecular compositions in Peru Margin sediments. *Geochimica et Cosmochimica Acta* **61**, 1247–60.

Bhushan R, Dutta K and Somayajulu BLK (2001) Concentrations and burial fluxes of organic and inorganic carbon on the eastern margins of the Arabian Sea. *Marine Geology* **178**, 95–113.

Blaauw M and Christen JA (2011) Flexible paleoclimate age-depth models using an autoregressive gamma process. *Bayesian Analysis* **6**, 457–74.

Böll A, Lückge A, Munz P, Forke S, Schulz H, Ramaswamy V, Rixen T, Gaye B and Emeis K-C (2014) Late Holocene primary productivity and sea surface temperature variations in the northeastern Arabian Sea: implications for winter monsoon variability. *Paleoceanography* **29**, 778–94.

Brady PV (1991) The effect of silicate weathering on global temperature and atmospheric CO2. Journal of Geophysical Research 96, 101–18.

Burdanowitz N, Gaye B, Hilbig L, Lahajnar N, Lückge A, Rixen T and Emeis K-C (2019) Holocene monsoon and sea level-related changes of sedimentation in the northeastern Arabian Sea. *Deep Sea Research* **66**, 6–18.

Cai W-J, Hu X, Huang W-J, Murrell MC, Lehrter JC, Lohrenz SE, Chou W-C, Zhai W, Hollibaugh JT, Wang Y, Zhao P, Guo X, Gundersen K, Dai M and Gong G-C (2011) Acidification of subsurface coastal waters enhanced by eutrophication. *Nature Geoscience* **4**, 766–70.

Calvert SE, Pedersen TF, Naidu PD and Von Stackelberg U (1995) On the organic carbon maximum on the continental slope of the eastern Arabian Sea. *Journal of Marine Research* **53**, 269–96.

Carlson CA, Bates NR, Hansell DA and Steinberg DK (2001) Carbon cycle. In *Encyclopedia of Ocean Sciences*, 2nd edn (eds J Steele, S Thorpe and K Turekian), 477–86. Academic Press.

Chadwick AJ and Lamb MP (2021) Climate-change controls on river delta avulsion location and frequency. *Journal of Geophysical Research: Earth Surface* **126**, e2020JF005950.

Chandramohan P, Jena BK and Sanilkumar V (2001) Littoral drift sources and sinks along the Indian coast. *Current Science* **81**, 292–7.

Ciais P, Sabine C, Bala G, Bopp L, Brovkin V, Canadell J, Chhabra A, DeFries R, Galloway J, Heimann M, Jones C, Le Quéré C, Myneni RB, Piao S and Thornton P (2013) Carbon and other biogeochemical cycles. In *Climate Change 2013: The Physical Science Basis. Contribution of Working Group I to the Fifth Assessment Report of the Intergovernmental Panel on Climate Change* (eds TF Stocker, D Qin, G-K Plattner, M Tignor, SK Allen, J Boschung, A Nauels, Y Xia, V Bex and PM Midgley), 465–570. Cambridge and New York: Cambridge University Press.

Diniz JE, Nayak GN, Noronha-D'Mello CA and Mishra R (2018) Reconstruction of palaeo-depositional environment in north-eastern Arabian Sea. *Environmental Earth Sciences* **77**, 665.

Dixit Y, Hodell DA and Petrie CA (2014) Abrupt weakening of the summer monsoon in northwest India ~4100 yr ago. *Geology* **42**, 339–42.

Dutta K, Bhushan R and Somayajulu BLK (2001) ΔR correction values for the Northern Indian Ocean. *Radiocarbon* **43**, 483–8.

Enzel Y, Ely LL, Mishra S, Ramesh R, Amit R, Lazar B, Rajaguru SN, Baker VR and Sandle A (1999) High-resolution Holocene environmental changes in the Thar Desert, northwestern India. *Science* **284**, 125–8.

Falkowski P, Scholes RJ, Boyle E, Canadell J, Canfield D, Elser J, Gruber N, Hibbard K, Högberg P, Linder S, Mackenzie FT, Moore III B, Pedersen T, Rosenthal Y, Seitzinger S, Smetacek V and Steffen W (2000) The global carbon cycle: a test of our knowledge of earth as a system. *Science* **290**, 291–6.

Field CB, Behrenfeld MJ, Randerson JT and Falkowski P (1998) Primary production of the biosphere: integrating terrestrial and oceanic components. *Science* **281**, 237–40.

Freitas FS, Arndt S, Hendry KR, Faust JC, Tessin AC and März C (2022) Benthic organic matter transformation drives pH and carbonate chemistry in Arctic marine sediments. *Global Biogeochemical Cycles*, **36**, e2021GB007187.

Gadgil S and Kumar KR (2006) The Asian monsoon-agriculture and economy. In *The Asian Monsoon*, pp. 651–83. Berlin and Heidelberg: Springer.

Galy V, France-Lanord C, Beyssac O, Faure P, Kudrass H-R and Palhol F (2007) Efficient organic carbon burial in the Bengal fan sustained by the Himalayan erosional system. *Nature* **450**, 407–11.

Grant KM, Rohling EJ, Ramsey CB, Cheng H, Edwards RL, Florindo F, Heslop D, Marra F, Roberts AP, Tamisiea ME and Williams F (2014) Sea-level variability over five glacial cycles. *Nature Communications* **5**, 5076.

Gupta AK, Anderson DM and Overpeck JT (2003) Abrupt changes in the Asian southwest monsoon during the Holocene and their links to the North Atlantic Ocean. *Nature* **421**, 354–7.

Guptha MVS, Curry WB, Ittekkot V and Muralinath AS (1997) Seasonal variation in the flux of planktic foraminifera: sediment trap results from the Bay of Bengal, Northern Indian Ocean. *Journal of Foraminiferal Research* **27**, 5–19.

Guptha MVS, Naidu PD, Haake BG and Schiebel R (2005) Carbonate and carbon fluctuations in the eastern Arabian Sea over 140 ka: implications on productivity changes? *Deep Sea Research* **52**, 1981–93.

Haake B, Ittekkot V, Rixen T, Ramaswamy V, Nair RR and Curry WB (1993) Seasonality and interannual variability of particle fluxes to the deep Arabian Sea. *Deep-Sea Research* **40**, 1323–44.

Hashimi NH, Kidwai RM and Nair RR (1981) Comparative study of the topography and sediments of the western and eastern continental shelves around Cape Comorin. *Indian Journal of Geo-Marine Science* **10**, 45–50.

Hashimi NH, Nair RR, Kidwai RM and Purnachandra Rao V (1982) Carbonate mineralogy and faunal relationship in tropical shallow water marine sediments: Cape Comorin, India. *Sedimentary Geology* **32**, 89–98.

IPCC (2021) Summary for policymakers. In *Climate Change 2021: The Physical Science Basis. Contribution of Working Group I to the Sixth Assessment Report of the Intergovernmental Panel on Climate Change* (V Masson-Delmotte, P Zhai, A Pirani, SL Connors, C Péan, S Berger, N Caud, Y Chen, L Goldfarb, MI Gomis, M Huang, K Leitzell, E Lonnoy, JBR Matthews, TK Maycock, T Waterfield, O Yelekçi, R Yu and B Zhou), 3−32. Cambridge, UK and New York, NY, USA: Cambridge University Press.

Jagadeesan L, Jyothibabu R, Anjusha A, Mohan AP, Madhu NV, Muraleedharan KR and Sudheesh K (2013) Ocean currents structuring the mesozooplankton in the Gulf of Mannar and the Palk Bay, southeast coast of India. *Progress in Oceanography* **110**, 27–48.

Jasper JP and Gagosian RB (1989) Glacial–interglacial climatically forced $\delta^{13}C$ variations in sedimentary organic matter. *Nature* **342**, 60–2.

Johnson JE, Phillips SC, Torres ME, Piñero E, Rose KK and Giosan L (2014) Influence of total organic carbon deposition on the inventory of gas hydrate in the Indian continental margins. *Marine and Petroleum Geology* **58**, 406–24.

Jyothibabu R, Asha Devi CR, Madhu NV, Sabu P, Jayalakshmy KV, Jacob J, Habeebrehman H, Prabhakaran MP, Balasubramanian T and Nair KKC (2008) The response of microzooplankton (20–200 mm) to coastal upwelling and summer stratification in the southeastern Arabian Sea. *Continental Shelf Research* **28**, 653–71.

Jyothibabu R, Balachandran KK, Jagadeesan L, Karnan C, Gupta GVM, Chakraborty K and Sahu KC (2021) Why the Gulf of Mannar is a marine biological paradise? *Environmental Science and Pollution Research* **28**, 64892–907.

Kaminski MA and Kuhnt W (1995) Tubular agglutinated foraminifera as indicators of organic carbon flux. In *Proceedings of the Fourth International Workshop on Agglutinated Foraminifera* (eds MA Kaminski, S Geroch, MA Gasinski), pp. 141–4. Grzybowski Foundation Special Publication no. 3.

Keil R (2017) Anthropogenic forcing of carbonate and organic carbon preservation in marine sediments. *Annual Review of Marine Science* **9**, 151–72.

Kessarkar PM and Rao VP (2007) Organic carbon in sediments of the southwestern margin of India: influence of productivity and monsoon variability during the Late Quaternary. *Journal of the Geological Society of India* **69**, 42–52.

Kessarkar PM, Rao VP, Naqvi SWA, Chivas AR and Saino T (2010) Fluctuations in productivity and denitrification in the southeastern Arabian Sea during the Late Quaternary. *Current Science* **99**, 485–91.

Khare N (2018) Evidence of increased rainfall prior to 3500 years BP as revealed by river borne terrigenous flux: a study from west coast of India. *Quaternary International* **479**, 100–5.

Khare N, Nigam R and Hashimi NH (2008) Revealing monsoonal variability of the last 2,500 years over India using sedimentological and foraminiferal proxies. *Facies* **54**, 167–73.

Kolla V, Ray PK and Kostecki JA (1981) Surficial sediments of the Arabian Sea. *Marine Geology* **41**, 183–204.

Kotlia BS, Singh AK, Joshi LM and Dhaila BS (2015) Precipitation variability in the Indian Central Himalaya during last ca. 4,000 years inferred from a speleothem record: impact of Indian Summer Monsoon (ISM) and Westerlies. *Quaternary International* **371**, 244–53.

Langer MR (2008) Assessing the contribution of foraminiferan protists to global ocean carbonate production. *Journal of Eukaryotic Microbiology* **55**, 163–9.

LaRowe DE, Arndt S, Bradley JA, Estes ER, Hoarfrost A, Lang SQ, Lloyd KG, Mahmoudi N, Orsij WD, Shah Walter SR, Steen AD and Zhao R (2020) The fate of organic carbon in marine sediments: new insights from recent data and analysis. *Earth-Science Reviews* **204**, 103146.

Locarnini RA, Mishonov AV, Baranova OK, Boyer TP, Zweng MM, Garcia HE, Reagan JR, Seidov D, Weathers K, Paver CR and Smolyar I (2018) *World Ocean Atlas 2018, Vol. 1: Temperature* (technical ed. A. Mishonov). Silver Spring, MD: National Oceanic and Atmospheric Administration. NOAA Atlas NESDIS, 81, 52 pp.

Lüthi D, Floch ML, Bereiter B, Blunier T, Barnola J-M, Siegenthaler U, Raynaud D, Jouzel J, Fischer H, Kawamura K and Stocker TF (2008) High-resolution carbon dioxide concentration record 650,000–800,000 years before present. *Nature* **453**, 379–82.

Madhupratap M, Prasanna Kumar S, Bhattathiri PMA, Dileep Kumar M, Raghu Kumar S, Nair KKC and Ramaiah N (1996) Mechanism of the biological response to winter cooling in the northeastern Arabian Sea. *Nature* **384**, 549–52.

Misra S and Froelich PN (2012) Lithium isotope history of Cenozoic seawater: changes in silicate weathering and reverse weathering. *Science* **335**, 818–23.

Nagoji SS and Tiwari M (2017) Organic carbon preservation in southeastern Arabian Sea sediments since mid-Holocene: implications to South Asian summer monsoon variability. *Geochemistry, Geophysics, Geosystems* **18**, 3438–51.

Naidu AS and Shankar R (1999) Palaeomonsoon history during the late Quaternary: results of a pilot study on sediments from the Laccadive Trough, southeastern Arabian Sea. *Journal of the Geological Society of India* **53**, 401–6.

Naidu PD (1991) Glacial to interglacial contrasts in the calcium carbonate content and influence of Indus discharge in two eastern Arabian Sea cores. *Palaeogeography, Palaeoclimatology, Palaeoecology* **86**, 255–63.

Naidu PD, Ramesh Kumar MR and Ramesh Babu V (1999) Time and space variations of monsoonal upwelling along the west and east coasts of India. *Continental Shelf Research* **19**, 559–72.

Naik DK, Saraswat R, Lea DW, Kurtarkar SR and Mackensen A (2017) Last glacial-interglacial productivity and associated changes in the eastern Arabian Sea. *Palaeogeography, Palaeoclimatology, Palaeoecology* **483**, 147–56.

Naik SS, Godad SP, Naidu PD, Tiwari M and Paropkari AL (2014) Early to late-Holocene contrast in productivity, OMZ intensity and calcite dissolution in the eastern Arabian Sea. *The Holocene* **24**, 749–55.

Nair RR, Ittekkot V, Manganini SJ, Ramaswamy V, Haake B, Degens ET and Honjo S (1989) Increased particle flux to the deep ocean related to monsoons. *Nature* **338**, 749–51.

Narayana AC, Naidu PD, Shinu N, Nagabhushanam P and Sukhija BS (2009) Carbonate and organic carbon content changes over last 20 ka in the southeastern Arabian Sea: paleoceanographic implications. *Quaternary International* **206**, 72–7.

Olausson E (1971) Quaternary correlations and the geochemistry of oozes. In *The Micropaleontology of Oceans* (ed BM Funnel), pp. 375–98. Cambridge: Cambridge University Press.

Paropkari AL, Babu CP and Mascarenhas A (1992) A critical evaluation of depositional parameters controlling the variability of organic carbon in Arabian Sea sediments. *Marine Geology* **107**, 213–26.

Pattan JN, Masuzawa T, Naidu PD, Parthiban G and Yamamoto M (2003) Productivity fluctuations in the southeastern Arabian Sea during the last 140 ka. *Palaeogeography, Palaeoclimatology, Palaeoecology* **193**, 575–90.

Pattan JN, Parthiban G and Amonkar A (2019) Productivity controls on the redox variation in the southeastern Arabian Sea sediments during the past 18 kyr. *Quaternary International* **523**, 1–9.

Phillips JD and Slattery MC (2006) Sediment storage, sea level, and sediment delivery to the ocean by coastal plain rivers. *Progress in Physical Geography* **30**, 513–30.

Prasanna Kumar S, Madhupratap M, Dileepkumar M, Muraleedharan P, DeSouza S, Gauns M and Sarma V (2001) High biological productivity in the central Arabian Sea during the summer monsoon driven by Ekman pumping and lateral advection. *Current Science* **81**, 1633–8.

Prell WL and Curry WB (1981) Faunal and isotopic indices of monsoonal upwelling: western Arabian Sea. *Oceanologica Acta* **4**, 91–8.

Ramaswamy V and Gaye B (2006) Regional variations in the fluxes of foraminifera carbonate, coccolithophorid carbonate and biogenic opal in the northern Indian Ocean. *Deep-Sea Research I* **53**, 271–93.

Ramaswamy V and Nair RR (1994) Fluxes of material in the Arabian Sea and Bay of Bengal: sediment trap studies. *Proceedings of the Indian Academy of Sciences (Earth and Planetary Sciences)* **103**, 189–210.

Rao VP, Rajagopalan G, Vora KH and Almeida F (2003) Late Quaternary sea level and environmental changes from relic carbonate deposits of the western margin of India. *Proceedings of the Indian Academy of Sciences (Earth and Planetary Sciences)* **112**, 1–25.

Ray SB, Rajagopalan G and Somayajulu BLK (1990) Radiometric studies of sediments cores from Gulf of Mannar. *Indian Journal of Marine Science* **19**, 9–12.

Raymo ME and Ruddiman WF (1992) Tectonic forcing of Late Cenozoic climate. *Nature* **359**, 117–22.

Reichart GJ, Schenau SJ, de Lange GJ and Zachariasse WJ (2002) Synchroneity of oxygen minimum zone intensity on the Oman and Pakistan Margins at sub-Milankovitch time scales. *Marine Geology* **185**, 403–15.

Reimer PJ, Bard E, Bayliss A, Beck JW, Blackwell PG, Bronk-Ramsey C, Buck CE, Cheng H, Edwards RL, Friedrich M, Grootes PM, Guilderson TP, Haflidason H, Hajdas I, Hatté C, Heaton TJ, Hogg AG, Hughen KA, Kaiser KF, Kromer B, Manning SW, Niu M, Reimer RW, Richards DA, Scott EM, Southon JR, Turney CSM and van der Plicht J (2013) IntCal13 and MARINE13 radiocarbon age calibration curves 0–50000 years calBP. *Radiocarbon* **55**, 1869–87.

Saalim SM, Saraswat R, Suokhrie T and Nigam R (2019) Assessing the ecological preferences of agglutinated benthic foraminiferal morphogroups from the western Bay of Bengal. *Deep-Sea Research Part II*, **161**, 38–51.

Salter I, Schiebel R, Ziveri P, Movellan A, Lampitt R and Wolff GA (2014) Carbonate counter pump stimulated by natural iron fertilization in the Polar Frontal Zone. *Nature Geoscience* **7**, 885–9.

Sanwal J, Kotlia BS, Rajendran CP, Ahmad SM, Rajendran K and Sandiford M (2013) Climatic variability in Central Indian Himalaya during the last ~1,800 years: evidence from high resolution speleothem record. *Quaternary Research* **304**, 183–92.

Saraswat R (2015) Non-destructive foraminiferal paleoclimatic proxies: a brief insight. *Proceedings of the Indian National Science Academy* **81**, 381–95.

Saraswat R an Khare N (2010) Deciphering the calcification depth of *Globigerina bulloides* from its oxygen isotopic composition. *Journal of Foraminiferal Research* **40**, 220–30.

Saraswat R, Kurtarkar SR, Yadav R, Mackensen A, Singh DP, Bhadra S, Singh AD, Tiwari M, Prabhukeluskar SP, Bandodkar SR, Pandey DK, Clift PD, Kulhanek DK, Bhishekar K and Nair S (2020) Inconsistent change in surface hydrography of the northeastern Arabian Sea during the last four glacial–interglacial intervals. *Geological Magazine* **157**, 989–1000.

Saraswat R, Naik DK, Nigam R and Gaur AS (2016) Timing, cause and consequences of mid-Holocene climate transition in the Arabian Sea. *Quaternary Research* **86**, 162–9.

Saravanan P, Gupta AK, Zheng H, Panigrahi MK and Prakasam M (2019) Late Holocene long arid phase in the Indian subcontinent as seen in shallow sediments of the eastern Arabian Sea. *Journal of Asian Earth Science* **181**, 103915.

Sarkar A, Ramesh R, Somayajulu BLK, Agnihotri R, Jull AJT and Burr GS (2000) High resolution Holocene monsoon record from the eastern Arabian Sea. *Earth and Planetary Science Letters* **177**, 209–18.

Sarma VVSS, Dileep Kumar M and Saino T (2007) Impact of sinking carbon flux on accumulation of deep-ocean carbon in the Northern Indian Ocean. *Biogeochemistry* **82**, 89–100.

Sarma VVSS, Udaya Bhaskar TVS, Kumar JP and Chakraborty K (2020) Potential mechanisms responsible for occurrence of core oxygen minimum zone in the north-eastern Arabian Sea. *Deep Sea Research* **165**, 103393.

Schiebel R (2002) Planktic foraminiferal sedimentation and the marine calcite budget. *Global Biogeochemical Cycles* **16**, 1065.

Schiebel R, Waniek J, Bork M and Hemleben CH (2001) Planktic foraminiferal production stimulated by chlorophyll redistribution and entrainment of nutrients. *Deep-Sea Research Part I* **48**, 721–40.

Schott FA and McCreary Jr JP (2001) The monsoon circulation of the Indian Ocean. *Progress in Oceanography* **51**, 1–123.

Singh DP, Saraswat R and Kaithwar A (2018) Changes in standing stock and vertical distribution of benthic foraminifera along a depth gradient (58–2750 m) in the southeastern Arabian Sea. *Marine Biodiversity* **48**, 73–88.

Singh DP, Saraswat R and Naik DK (2017) Does glacial-interglacial transition affect sediment accumulation in monsoon dominated regions? *Acta Geologica Sinica* **91**, 1079–94.

Southon J, Kashgarian M, Fontugne M, Metivier B and Yim WW-S (2002) Marine reservoir corrections for the Indian Ocean and Southeast Asia. *Radiocarbon* **44**, 167–80.

Sreeush MG, Valsala V, Pentakota S, Prasad KVSR and Murtugudde R (2018) Biological production in the Indian Ocean upwelling zones – Part 1: refined estimation via the use of a variable compensation depth in ocean carbon models. *Biogeosciences* **15**, 1895–918.

Srivastava P, Agnihotri R, Sharma D, Meena N, Sundriyal YP, Saxena A, Bhushan R, Sawlani R, Banerji US, Sharma C, Bisht P, Rana N and Jayangondaperumal R (2017) 8000-year monsoonal record from Himalaya revealing reinforcement of tropical and global climate systems since mid-Holocene. *Scientific Reports* **7**, 14515.

Staubwasser M and Sirocko F (2001) On the formation of laminated sediments on the continental margin off Pakistan: the effects of sediment provenance and sediment redistribution. *Marine Geology* **172**, 43–56.

Staubwasser M, Sirocko F, Grootes PM and Segl M (2003) Climate change at the 4.2 ka BP termination of the Indus Valley civilization and Holocene South Asian monsoon variability. *Geophysical Research Letters* **30**, 1425.

Stuiver M and Reimer PJ (1993) Extended ^{14}C data base and revised CALIB 3.0 ^{14}C age calibration program. *Radiocarbon* **35**, 215–30.

Sulochanan B and Muniyandi K (2005) Hydrographic parameters off Gulf of Mannar and Palk Bay during a year of abnormal rainfall. *Journal of the Marine Biological Association of India* **47**, 198–200.

Thamban M, Rao VP and Raju SV (1997) Controls on organic carbon distribution in sediments from the eastern Arabian Sea margin. *Geo-Marine Letters* **17**, 220–7.

Thomas LC, Padmakumar KB, Smitha BR, Devi CA, Nandan SB and Sanjeevan VN (2013) Spatio-temporal variation of microphytoplankton in the upwelling system of the south-eastern Arabian Sea during the summer monsoon of 2009. *Oceanologia* **55**, 185–204.

Vinayachandran PN and Mathew S (2003) Phytoplankton bloom in the Bay of Bengal during the northeast monsoon and its intensification by cyclones. *Geophysical Research Letters* **30**, 1572.

von Rad U, Schulz H, Riech V, den Dulk M, Berner U and Sirocko F (1999) Monsoon-controlled breakdowns of oxygen-minimum conditions during the past 30,000 years documented in laminated sediments off Pakistan. *Palaeogeography, Palaeoclimatology, Palaeoecology* **152**, 129–61.

Wan S, Clift PD, Li A, Yu Z, Li T and Hu D (2012) Tectonic and climatic controls on long-term silicate weathering in Asia since 5 Ma. *Geophysical Research Letters* **39**, L15611.

Weber ME, Lantzsch H, Dekens P, Das SK, Reilly BT, Martos YM, Meyer-Jacob C, Agrahari S, Ekblad A, Titschack J, Holmes B and Wolfgramm P

(2018) 200,000 years of monsoonal history recorded on the lower Bengal Fan – strong response to insolation forcing. *Global and Planetary Change* **166**, 107–19.

Xu Z, Wan S, Colin C, Clift PD, Chang F, Li T, Chen H, Cai M, Yu Z and Lim D (2021) Enhancements of Himalayan and Tibetan erosion and the produced organic carbon burial in distal tropical marginal seas during the Quaternary glacial periods: an integration of sedimentary records. *Journal of Geophysical Research: Earth Surface* **126**, e2020JF005828.

Zeebe RE and Wolf-Gladrow DA (2001) *CO_2 in Seawater: Equilibrium, Kinetics, Isotopes*. Elsevier Oceanography Series, vol. **65**. Amsterdam: Elsevier, 346 pp.

Zweng MM, Reagan JR, Seidov D, Boyer TP, Locarnini RA, Garcia HE, Mishonov AV, Baranova OK, Weathers K, Paver CR and Smolyar I (2018) *World Ocean Atlas 2018, Vol. 2: Salinity* (technical ed. A. Mishonov). Silver Spring, MD: National Oceanic and Atmospheric Administration. NOAA Atlas NESDIS, 82, 50 pp.